AN ABSTRACT OF THE THESIS OF

Lucian Chis for the degree of Master of Science in

Electrical and Computer Engineering presented on August 24, 1998.

Title: Testing and Modeling of the Single-Phase Written-Pole Motor

Redacted for Privacy

Abstract approved: _____

Alan Wallace

A relatively new development in the electric machines field has been the written-pole technology, of which the latest product is the large single-phase electric motor, the single phase Written-Pole Motor (WPM). The WPM is a synchronous, permanent-magnet single-phase motor having a weak rotor cage for start-up which in addition exhibits significant hysteresis effects at speeds below or above true synchronism. The electrical configuration of the WPM places it in the capacitor-start capacitor-run category of single-phase motors, due to the large size and need for an approximation of a round rather than elliptic rotating magnetic field.

This thesis presents the results of the research conducted by the author in the Motor Systems Resource Facility (MSRF) of the Electrical and Computer Engineering Department at Oregon State University. The thesis is structured into two main parts: Testing and Modeling.

The tests conducted on the WPM were trying to independently verify manufacturer's claims with regards to efficiency, power factor, robustness, power-outage ride-through and furthermore to study the behaviour of the machine during voltage sags, overvoltages and undervoltages. Tests were conducting in order to develop a

mathematical model from which the performance of the machine can be predicted.

The modeling efforts were concentrated in the development of a comprehensive model which would include all three major aspects of the WPM, and the performance of the resulting model was compared with the sampled data.

Testing and Modeling of the Single-Phase Written-Pole Motor

by

Lucian Chis

A THESIS

submitted to

Oregon State University

in partial fulfillment of
the requirements for the
degree of

Master of Science

Completed August 24, 1998
Commencement June 1999

Master of Science thesis of Lucian Chis presented on August 24, 1998

APPROVED:

Redacted for Privacy

Major Professor, representing Electrical and Computer Engineering

Redacted for Privacy

Chair of the Department of Electrical and Computer Engineering

Redacted for Privacy

Dean of the Graduate School

I understand that my thesis will become part of the permanent collection of Oregon State University libraries. My signature below authorizes release of my thesis to any reader upon request.

Redacted for Privacy

Lucian Chis, Author

TABLE OF CONTENTS

TABLE OF CONTENTS (Continued)

TABLE OF CONTENTS (Continued)

LIST OF FIGURES

TESTING AND MODELING OF THE SINGLE-PHASE WRITTEN-POLE MOTOR

1. INTRODUCTION

1.1. Overview of the Written-Pole Technology

Precise Power Corporation's "Written-Pole" technology has been emerging for some time in the field of Uninterruptable Power Supplies, three-phase motor-generator sets (Roessel Motor-Generators) and others [13]. The latest offshoot of this technology is the large single phase "Written-Pole Motor" [11]. Conventional single-phase motors, typically using a capacitor-start/capacitor run induction machine configuration as shown in Fig 1.1, are generally limited to applications requiring less than 5kW, at 240V. One reason for this limitation is the starting current, which is typically 6 to 10 times the rated current of the machine. This magnitude of the current can cause voltage sag or flicker conditions for other equipment, especially in weak lines found in remote locations as farms, small mines, and recreational facilities fed by long lines having an appreciable equivalent source impedance. In order to satisfy larger loads, such as pumps and fans without the prohibitive construction cost of three-phase distribution systems, several alternatives have been proposed [1]. The Written-Pole motor joins these ranks besides the following options: operation of a conventional three-phase induction motor via a single-phase to three-phase power converter (i.e. a modified adjustable speed drive) with soft start capability; operation of a conventional three-phase motor from a single-phase supply via a "semi-hex" connection, as developed by Smith [10]. The Written-Pole single phase motor (WPM) is the result of the research and development of Precise

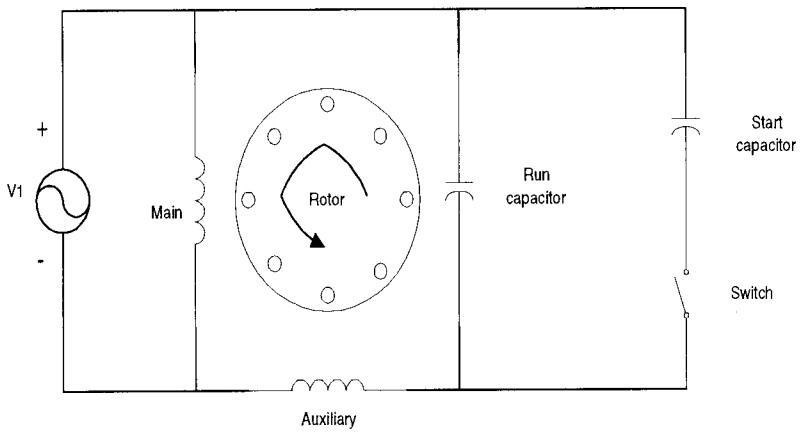

FIGURE 1.1: Typical Capacitor-Start Capacitor-Run Single-Phase Motor

Power Corporation with funding from a group of North American power utilities, under the auspices of the Electric Power Research Institute (EPRI), in response to the changing requirements of their remotely located customers. The range of powers initially envisioned for these motors was 15 to 60 kW.

A 20hp Written-Pole motor, having the nameplate data given in Appendix 1, was obtained for independent study and testing at the Motor Systems Resource Facility (MSRF) of Oregon State University (OSU).

The MSRF study was intended to complement and add to an earlier evaluation by Manitoba Hydro [4]. The Manitoba Hydro team studied the run-up and normal synchronous operation performance of an 1800rev/min machine in order to verify the manufacturer's claims.

The study presented here seeks to confirm the Manitoba Hydro findings and in addition investigates other WPM features such as performance during voltage sags, power outages, supply voltage variation effects . Also, a series of tests were performed in order to determine machine parameters, leading to an appropriate uni-

tary model of the WPM for performance prediction, since no analyses of this type are available in the published literature.

1.2. Single-Phase Written-Pole Motor Configuration

In order to operate from a single-phase supply, the WPM, as most single-phase motors of high power rating, emulates a balanced two-phase stator machine system which is required to develop a rotating magnetic field without undue counter rotating component. This arrangement is shown in the schematic of Fig 1.1. This represents a two-phase quadrature-winding arrangement with both switched (start) and permanent (run) capacitors which approximate a balanced operation during starting and running. In addition to this conventional stator configuration, several unique features have been incorporated into the machine in order to meet specific performance requirements. Several of these features are evident from a cross-sectional diagram of Fig 1.2:

1. In order to limit the line current during start-up, the WPM has a high-resistance cage rotor and a long effective air gap. The mechanical rotor-stator clearance of the WPM is similar to that of a conventional machine of the same size: the long magnetic "air" gap is due to a layer of ferrite, having a low relative permeability, attached to the rotor surface facing the stator. During start-up the ferrite exhibits a small amount of permanent magnetization which can not be completely erased by the rotating magnetic field, which is residual from previous operation. This layer is responsible for the greater part of a hysteresis torque which augments the induction torque of the rotor cage during starting, given the low flux densities the rotor laminations are subjected to.

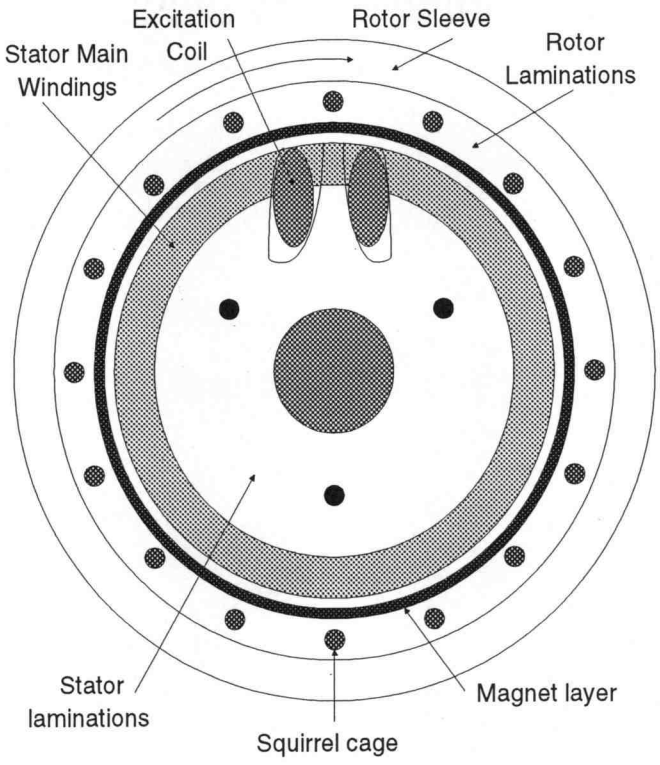

FIGURE 1.2: Written-Pole Motor Structure Schematic

2. In order to provide high efficiency and good power factor, the WPM operates as a synchronous permanent magnet machine under normal operating conditions. This is ingeniously achieved by "writing" "permanent" magnetic poles onto the ferrite layer by employing a special additional stator coil. This unusual stator coil, having a very small pitch is referred to, by the manufacturer, as the "excitation coil".

3. In order to avoid severe transients between the induction/hysteresis run-up and the synchronous normal operation, magnetic poles are repeatedly written on the rotor ferrite layer. Below 3600rev/min, for our 2 pole 60Hz machine, the length of the poles being written is shorter than a true pole pitch. This

makes the motor operate synchronously at less than synchronous speeds. This has been achieved by applying the line frequency currents to the excitation coil, without any electronic power processing.

4. In order to provide a measure of ride-through capability during supply voltage disturbances, the WPM has a high inertia external rotor, having a double cup design.

5. The WPM operation is controlled and monitored by an Intel 8051 serial microcontroller. The software can be customized in order to meet specific loads during start-up or sudden overload. The addition of a serial port enables on-line remote monitoring and control.

The WPM offers the following claimed advantages over other single-phase designs:

1. The starting current of the WPM is only 2.1pu (per-unit) enabling its ratings to be 300 % to 600% higher than previous induction machines in remote single-phase applications, without undue disturbance to other equipment.

2. The WPM, being a permanent magnet synchronous machine, has a higher efficiency than comparably sized induction motors for loads exceeding 60 % of the rated load.

3. It has a very high leading power factor, up to about 115% of the rated load. This substantially exceeds in value the power factor of comparable induction machines at all loads.

4. The high inertia of the rotor has the advantage that the starting of the motor is very slow thus making the WPM ideal for pumping applications where water hammer can be a problem. The same inertia provides ride-through during power outages of up to 15 seconds.

The objectives of the test program described in this thesis were to examine these claims.

2. PROPOSED MODELS FOR THE WPM

From the beginning it is evident, by examining the structure of the WPM, that it has three major electric machine torque-producing components. These are the induction, hysteresis and synchronous components.

The same stator configuration is responsible for all three components, whereas the rotor elements contribute to them as follows:

1. The rotor cage is responsible for an asynchronous or induction motor component at any speed other than synchronous.

2. The rotor ferrite layer and its laminations are the cause of the hysteresis motor component which is again present at all speeds other than synchronous. Most of this component however is located in the ferrite, which has a much larger area of the hysteresis loop compared to the laminations which are designed with a small hysteresis premise, operating at low flux densities (less than 1T). This conclusion is the result of the remanent flux density in the air gap at the synchronism being 0.4T as per manufacturer's data.

3. The rotor ferrite layer is responsible for the permanent magnet synchronous motor component at synchronism and in a speed range betweeen 80% and 100% of the rated speed (this range can be customized by changing the programming of the microcontroller). The writing, or excitation coil, located on the stator, is responsible for the appropriate magnetic pole configuration (i.e. the pole pitch) on the rotor.

2.1. Induction Motor Component

Between standstill and 80% of the rated speed (2880 rev/min in our particular case) the WPM has an induction component which derives from a high rotor cage resistance (steel conductors), high rotor leakage reactance (bars deeply set in the rotor laminations), and low magnetizing impedance (long electromagnetic gap). These features have the effect of (i) limiting the magnetization inrush current of the first cycle of the applied voltage, (ii) keeping the starting currents to a tolerable level and (iii) providing a high starting torque per amp ratio. Between standstill and full-speed a first capacitor switching is performed in order to maintain an approximation to balanced two-phase operation. A second capacitor switching takes place five seconds after synchronous speed operation has been attained. Due to the limited input power during start-up, and the high rotor inertia, the acceleration of the machine is very small. In consequence, the electrical time constants of the system are very small compared to the mechanical time constant of the machine and thus a transient or dynamic model of the WPM is unnecessary. Hence, the induction motor performance can be predicted by a steady-state equivalent circuit such as the one due to Veinott as shown in Fig 2.1, which accounts for the effects of both forward-rotating and backward-rotating field components of the unbalanced rotating magnetic field. However, in practice the WPM is substantially balanced by winding design and choice of capacitors, such that the conventional "per-phase" circuit may be adequate. Current and torque can be calculated by solving the circuit.

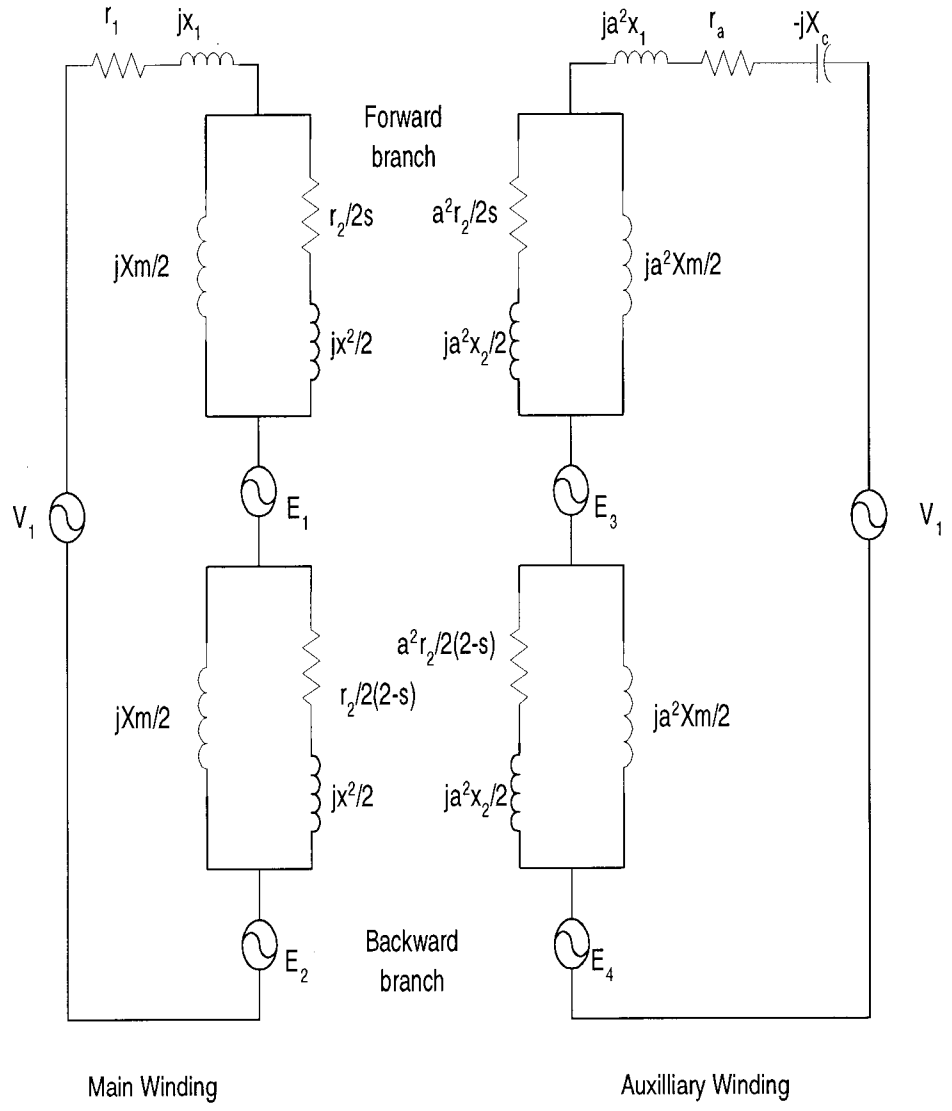

FIGURE 2.1: Extended Veinott Equivalent Circuit for the Single-phase Motor

2.2. Hysteresis Motor Component

The nature of the hysteresis torque rests in the fact that the magnetic field intensity (H) due to the stator windings, leads the resulting magnetic flux density (B) case, where the shape of the hysteresis loop is idealized as an ellipse or, more

realistically, the fundamental of the B waveform, by an angle ϕ_H [8]. In the general case, an eddy-curent component due to the electrical conductivity of the magnetic material would develop as well. The hysteresis component of the WPM is due mostly to the unmagnetized ferrite and therefore does not have any eddy-current component, because of the particular structure of the ferrite, which presents a high resistivity, due to its sinterized ferrous oxide structure. Also, the eddy-currents that appear in the rotor laminations are insignificant by design. In this case, were the WPM a balanced three-phase machine, the hysteresis torque would be constant throughout the speed range, having a value T_H given by [6]

$$T_H = \frac{A_h \times Vol \times p}{4\pi}, \tag{2.1}$$

in which A_H is the area of the hysteresis curve through which the material passes during each cycle, Vol is the volume of the ferrite, and p is the number of poles. It is to be remarked that during start-up the machine does not have a constant hysteresis. This is due, in a small amount, to the fact that the capacitors in the circuit seem to be overdesigned for the balanced two-phase operation (because the second step in the auxiliary circuit is only taken out 5 seconds after synchronism is attained). It is also due, in a larger amount, to the fact that, during the pole-writing mode, the poles are being fully magnetized for the first time and also an area that is dependent to the slip is being rewritten with a more or less different permanent magnetization. However, a major problem in estimating this component is finding the area of the hysteresis cycle which is followed by the ferrite, because the written poles from previous operation are not completely erased by the rotating magnetic field during all asynchronous operation. Thus in reality the ferrite is following minor hysteresis loops whose shape and size depend on the location relative to the last writing of the poles, which are effectivelly written in a sinusoidal fashion by the excitation coil

along the circumference of the rotor. The hysteresis component in general can be represented in a d-q equivalent circuit as a short-circuited winding in each circuit having a resistance to reactance ratio which is independent of the frequency (or slip) in acordance with the constant angle ϕ_H, and its resistance is inversely proportional to the slip, like an induction machine. In practice, the value of the torque can be calculated from the power dissipated in the equivalent resistance.

Determination of the necessary magnetic field information would require the use of a flux density probe or search coils to be inserted in the air gap of the WPM. This cannot be performed without irreversible modifications to the motor, which were not permitted in this investigation. Consequently, a matching technique was used to evaluate the hysteresis component of the torque and, from that, the the effective resistance for the equivalent circuit was obtained.

2.3. Synchronous Motor Component

When the WPM has attained 80% of the rated speed (synchronous) the micro-controller energizes the excitation coil and from this point forward the machine has a synchronous component. During the pole-writing mode the synchronous machine component is operating in an unusual manner: the power angle is constant, being dictated by the excitation coil spatial displacement with respect to the main stator coil. After the synchronous speed has been attained the poles are overwritten (there is actually an oversynchronous speed given by the negative slip of the rotor poles due to the position of the excitation pole) for another 5 seconds and then the excitation coil is deenergized and the dominant variable of the motor performance becomes the power angle, the machine behaving like a synchronous permanent magnet machine with a weak ammortiseur.

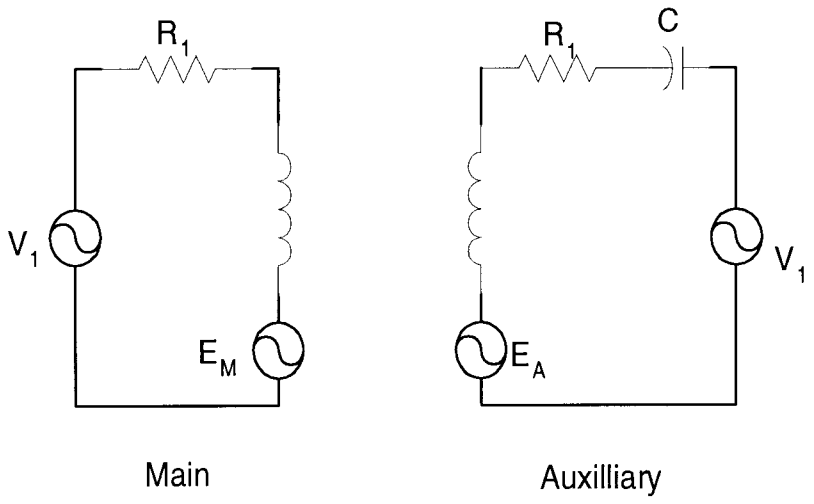

FIGURE 2.2: Single Phase PM Balanced Synchronous Machine Equivalent Circuit

In this mode of operation we can predict the torque by using the knowledge of the induced emfs.

$$T_S = \frac{I_M E_M + I_A E_A}{120\pi}, \tag{2.2}$$

in which E_M and E_A are the main and auxiliary induced emfs, and I_M and I_A are the respective currents for the WPM considered here (2 pole), as shown in Fig2.2.

3. TESTING OF THE WRITTEN-POLE MOTOR

The testing of the WPM was conducted in order to accomplish the following objectives:

1. First of all the system performance of the WPM needed to be evaluated through a thorough testing under different loads and supply voltage levels, during power outages, and supply voltage sags.

2. For the separation and quantization of the torque producing components of the WPM, which is required by an in depth understanding of this complex machine, a series of tests were devised, from which an appropriate equivalent circuit was obtained.

3. In order to obtain the parameters of the equivalent circuits of the individual torque producing components, short circuit, locked rotor, open circuit and no load, synchronous rotation tests were performed.

The testing of the WPM was accomplished using the resources of the Motor Systems Resource Facility of Oregon State University.

3.1. Overview of the MSRF Testing Facility.

The Motor Systems Resource Facility (MSRF) is a modern test and research facility funded by the Electric Power Research institute (EPRI) and Bonneville Power Administration (BPA) at the Electrical and Computer Engineering Department of Oregon State University. It has been designed as an industrial laboratory for standard motor tests as prescribed in the IEEE Standards 112 and 115 for polyphase induction and synchronous machines respectively, as well as testing of other kinds of

rotating or non-rotating electric machinery, adjustable speed drive systems, active and passive filters and general research in the field of electric machinery [2]. The MSRF has three test beds designed for machine ranges of up to 15hp, 75hp (under construction at this time) and up to 300hp for the large one. The large test bed of the Motor Systems Research Facility of Oregon State University was used for testing the WPM, due to the special nature of the testing required. This was dictated by the large inertia of the WPM and also by its physical size, both of which would place it in the 100hp range were it a standard induction machine.

3.2. The testing set-up

The large test bed of the MSRF can accommodate rotating electric machinery of up to 300hp and up to 4000rev/min and various tests can be performed employing a dynamometer which consists of a cage-rotor, inverter-grade induction machine fed by a four quadrant adjustable speed drive. The testing is done fully regeneratively, the only energy loss being due to the losses in the machine under test, the dynamometer machine and the power electronics conversion of the dynamometer converter. The dynamometer can be operated at this time in constant torque or constant speed modes. It has a speed transducer on its shaft and it has a torque estimator. The mechanical output or input of the machine under test is obtained through a strain gauge torque transducer (model 7540 made by Eaton-Lebow). Use of a Philips type PM6666 frequency counter enables measurement of the speed within hundreds of rev/min rather than just integral rev/min as obtainable from the Eaton-Lebow speed measurement. The electrical quantities of the machine under test are monitored through a Voltech type PMA 3300 true RMS power analyzer, which accepts also as auxiliary inputs the torque and speed as DC signals from

the Eaton-Lebow torque and speed transducer. The voltage was fed directly to the power analyzer whereas the currents were monitored through the use of Hall effect transducers (Model LT-500S by L.E.M.). These Hall effect Fig transducers have a distinct advantage over the regular shunts in that they provide galvanic isolation and at the same time are able to sense dc current components. The WPM was fed through two of the three computer regulated autotransformers available normally for three-phase testing configurations. The data can be remotely aquired through a parallel GP/IB bus through which the frequency counter and the power analyzer are connected to a computer equipped with the proper interface. In addition, during the testing, a Tektronix TDC460 four channel digitizing oscilloscope was used in order to obtain the time variation of torque, speed, current and voltage during "steady-state" and transients. Also the oscilloscope has waveform saving capability which has been used extensively during the course of the testing and research.

A schematic of the complete test system is shown in Fig 3.1.

3.3. Load tests

The bulk of the tests was done in order to verify manufacturer's claims with regard to the efficiency, power factor, inrush current magnitude, temperature rise, power outage ride-through, and robustness of the control circuit. Further tests were performed in order to analyze the effect of input voltage variations or sudden sags on WPM performance.

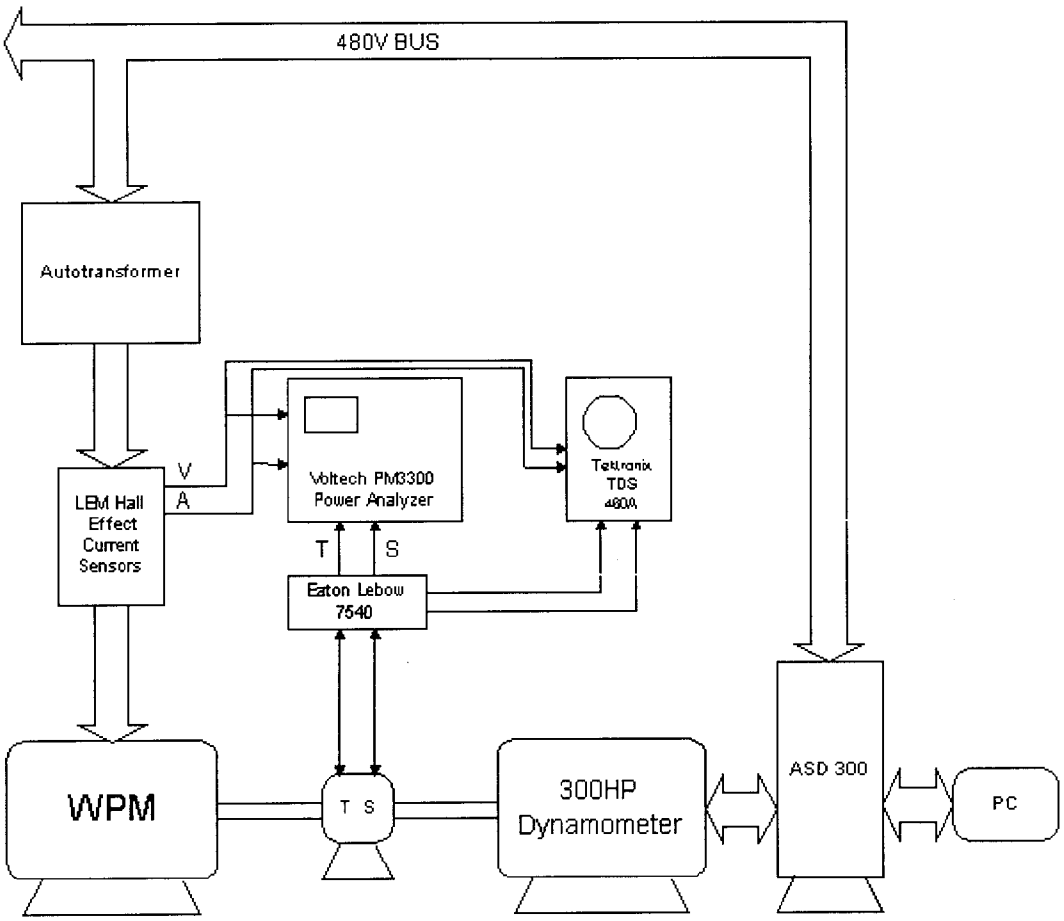

FIGURE 3.1: The Test Configuration

3.4. Starting Test.

For this test the WPM was connected to rated voltage in the configuration it was delivered which is the normal intended mode of operation. The current and torque during start-up were recorded on scope captures as shown in Fig 3.2. It has been found that the claims of the manufacturer with respect to the line current during start-up are justified, having recorded a starting current of 2.1pu. The cold WPM took an average of 57 seconds to start-up and synchronize working against the

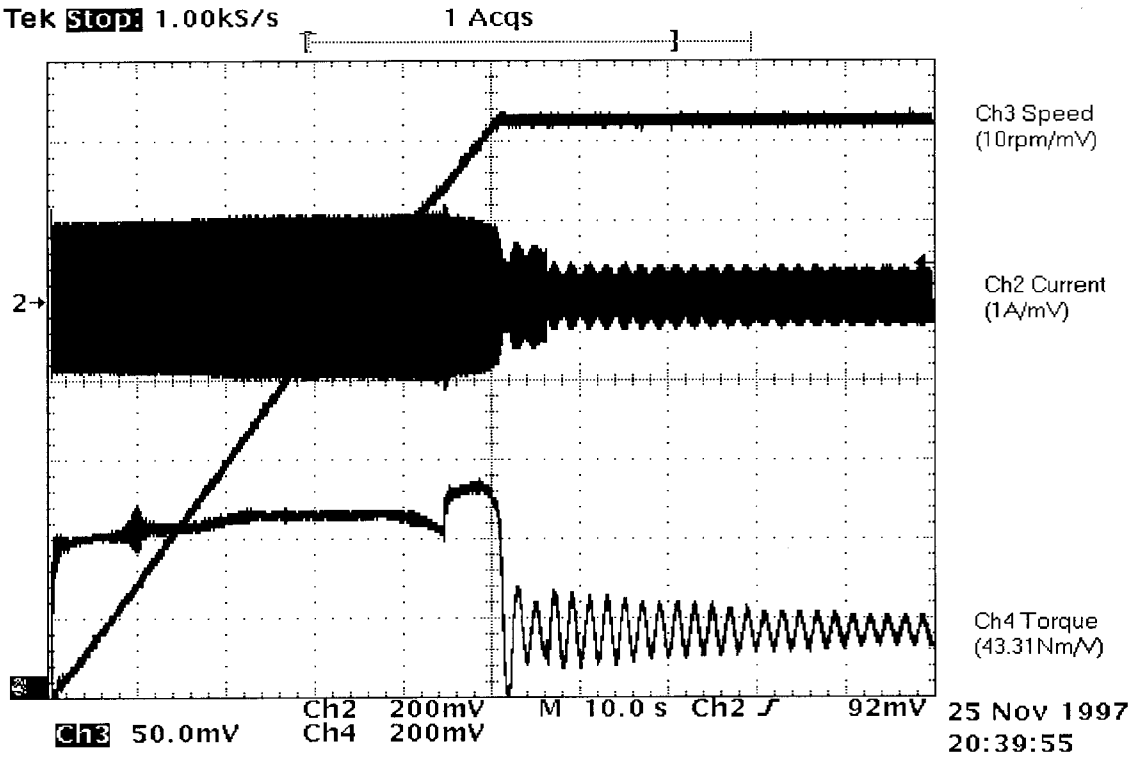

FIGURE 3.2: Net Torque Available, Line Current and Speed, during start-up

inertia, friction and windage of the test set consisting of itself and the dynamometer. The inertia of the WPM has to be figured in the estimation of the torque during start-up, given the very high polar moment of inertia (134.5 $lbft^2$ or $5.67kgm^2$). The acceleration during start-up is then almost constant having a value of about 7.25 rad/sec^2. This requires an acceleration torque of about 41.1 Nm which is not perceived at the shaft by the torque meter. This acceleration torque is very close to the rated torque of the machine so the oscilloscope capture of the torque during start-up shows the starting torque component in excess of the WPM rated torque.

It is discovered that the machine exhibits an appreciable cogging torque around 900 rev/min even after the smoothing action of the WPM inertia. This can be

attributed to a permanent magnet braking effect due to the previously written poles not being completely erased by the rotating magnetic field up to the respective speed. The starting characteristic also reveals the first capacitor switching which takes place around 2400rev/min. The beginning of the pole-writing process can be seen as a definite spike denoting the "catching" into synchronism while the machine still experiences induction and hysteresis torques. The second capacitor switching takes place immediately after proper synchronism is attained (5 seconds). The inertia corrected torque versus time characteristic can be used as the torque-speed characteristic with the appropriate scaling of the time axis (the speed is almost linear with time), because the mechanical time constant is a lot larger than the electrical ones.

3.5. WPM System load tests

The main part ot the test program was devoted to the load testing of the WPM.

3.5.1. Rated voltage tests

Since there are no relevant test procedures for this novel type of machine, a test program had to be designed by adapting the standard tests prescribed by IEEE Standards 112 and 115 for polyphase induction and synchronous machines respectively. During these tests, the machine was loaded at a particular level and the load kept constant until the WPM reached thermal stabilization. Because of the large thermal mass of the WPM compared to its ratings, this took approximately 6 hours for the rated load. The temperature of the windings of the WPM was monitored

through the internal temperature measurement devices with which the WPM was equipped from the factory. There are two sets of temperature measurement devices: a set of 4 thermistors which are monitored by the WPM microcontroller, one for each of the two phase stator windings and one for each of the excitation coils in the two halves of the machine. The WPM has redundant thermal protection having, in addition to these thermistors, a set of thermal cutouts in series in the control circuit input power.

A set of two thermocouples is available as well for field testing at the terminal box on the machine itself. The latter were connected to a Fluke handheld meter equipped with a thermocouple interface. The WPM microcontroller was connected through its serial port to a laptop computer operating in a VAX environment and so the temperatures measured by the internal thermistors were displayed along with a host of other useful information. Another temperature probe was used to measure the case temperature even though for this configuration of the WPM (external rotor) this information is less relevant.

The WPM during loaded or unloaded operation displays hunting or dynamic instability similar to that normally associated with an overexcited, underdamped synchronous machine coupled with a hysteresis type hunting effect. The amplitude of this hunting modulation of the available torque is itself time varying with a period of about 4 minutes. The two extremes are shown in Fig 3.3 and Fig 3.4. The torque and current waveforms were observed on the digitizing oscilloscope in order to get a qualitative measure of the modulating oscillation. In order to get meaningful results the minimum hunting condition has been chosen as the data aquisition point. The data was taken using the maximum number of averaging points available on the power analyser (64 readings were averaged over about 1 minute). There were 4 readings taken at each load and voltage points and their results averaged. A range

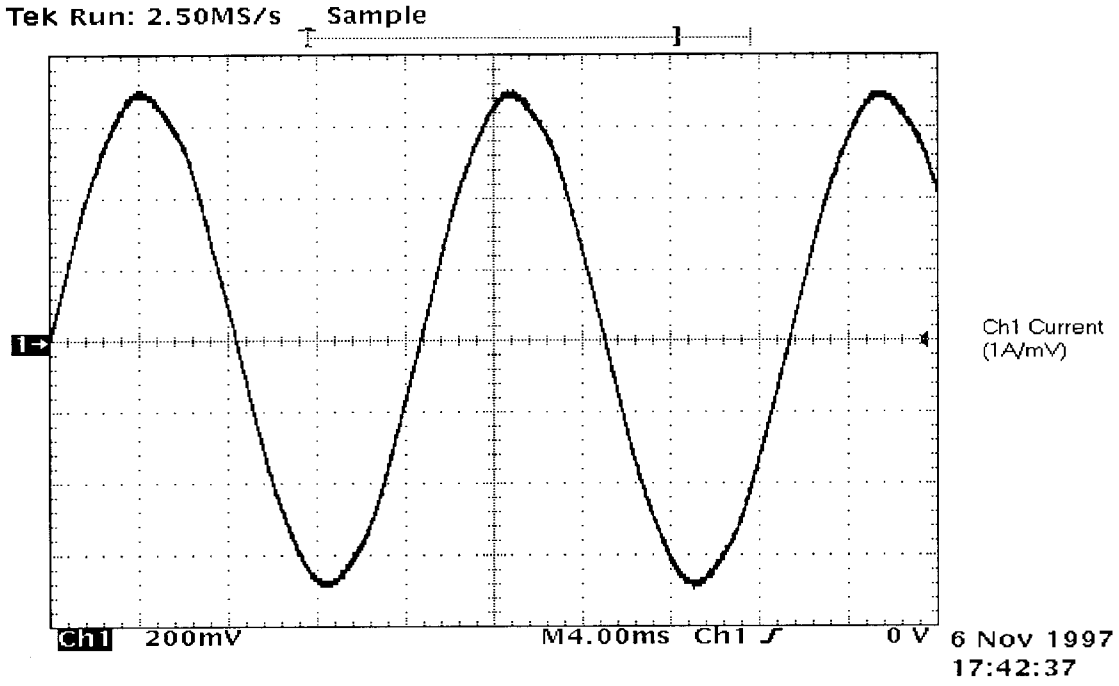

FIGURE 3.3: Maximum Amplitude Hunting Condition

of loads between 25% and 125% of the rated load were simulated first at the rated voltage and the resulting efficiency and power factor curves are presented in Fig 3.5 and Fig 3.6, respectively, along with typical induction motor respective curves for the same ratings. The WPM recommended overload is only 115% of the rated load, above which the motor reverts to the pole-writing mode in order to account for the excess load. This condition tends to overheat the rotor thus making it susceptible to a Curie point type loss of its magnetic properties.

It was found that the WPM was able to keep a 125% load stable during the testing. As is seen from the characteristics of Fig 3.5, the WPM has a higher efficiency than a typical induction motor of comparable ratings beginning from about 65% of its rating up to 125%.

This comparison doesn't take into account the fact that in the same type of

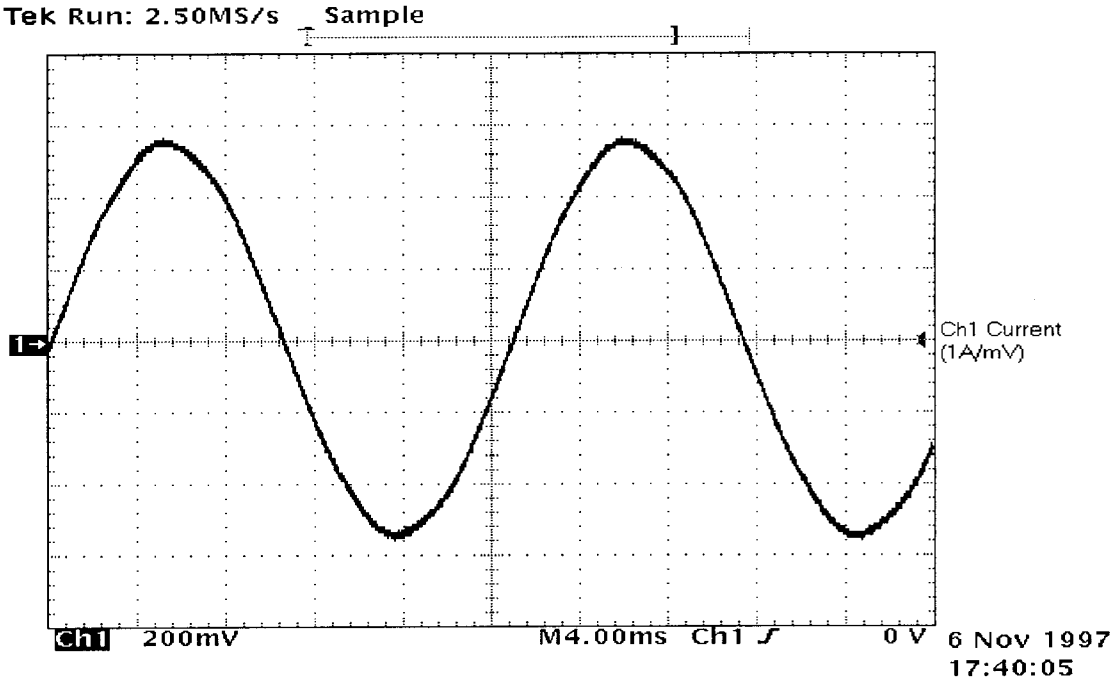

FIGURE 3.4: Minimum Amplitude Hunting Condition

applications (single-phase) the induction motor would be fed through an adjustable speed drive or a converter of some sort which would not have 100% efficiency.

As far as the power factor is concerned, the WPM outperforms the induction machine at all loads, as would be expected from a synchronous machine, as readily seen from Fig 3.6. As an added benefit, the power factor is leading up to about 120% of the rated load, from where it becomes lagging. As we shall see later, this benefit comes at the cost of dynamic instability or overstability.

3.5.2. Effect of Supply Voltage Variation on the Performance of WPM

In order to investigate the performance of the machine with the variation of the supply voltage, the load tests were repeated at 90% and 110% of the rated

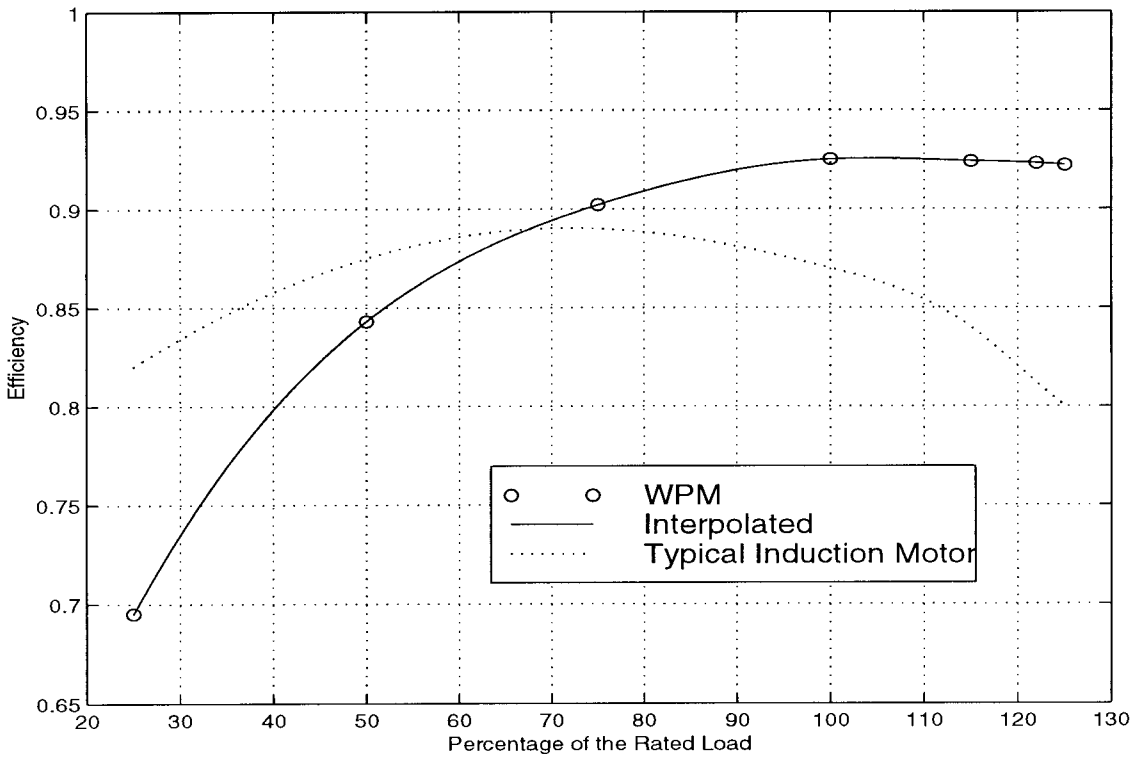

FIGURE 3.5: WPM and Typical 3-phase Induction Motor Efficiency

voltage. The results are presented in Fig 3.7 and Fig 3.8. It can be seen that the efficiency did vary slightly with the voltage throughout the load range, with minimal variation at the rated load and maximum at 50% load, hence it can be concluded that the voltage deviation from the rated value doesn't have a major impact on the efficiency. However, the power factor is affected strongly, especially at decreased loads, and its value is directly proportional to the value of the supply voltage.

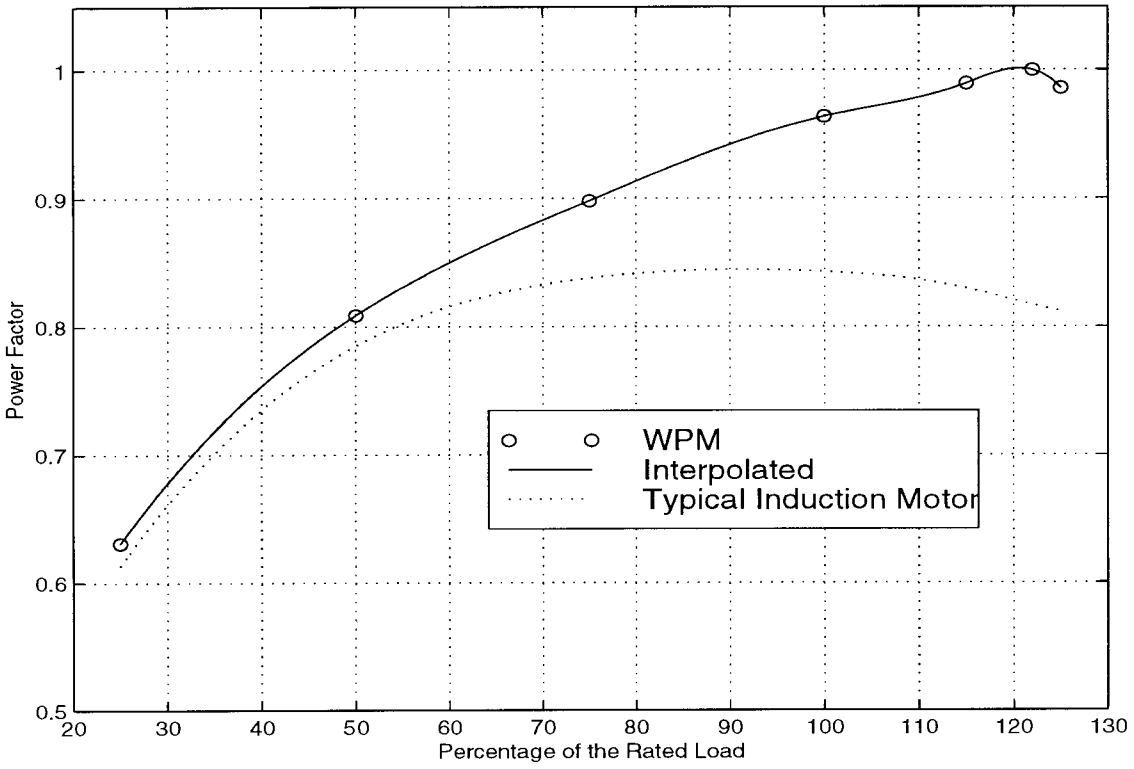

FIGURE 3.6: WPM and Typical 3-phase Induction Motor Power Factor

3.6. Restarting Test and Power Outage Simulation

It has been considered relevant for the performance analysis of the WPM to observe its behaviour when it was started at different coast-down speeds, at different loads. All these loads were handled well by the control software, which has energized the machine in the appropriate modes for the speeds and loads present. The most representative of these tests was the power outage test where the WPM, operating at full load in the constant torque mode of the dynamometer, was disconnected from the power supply for 15 seconds and then reconnected. The results are presented in the oscilloscope capture of Fig 3.9. As is seen from this oscilloscope capture, the inertia of the WPM covers the load requirements while its speed decreases to 2900

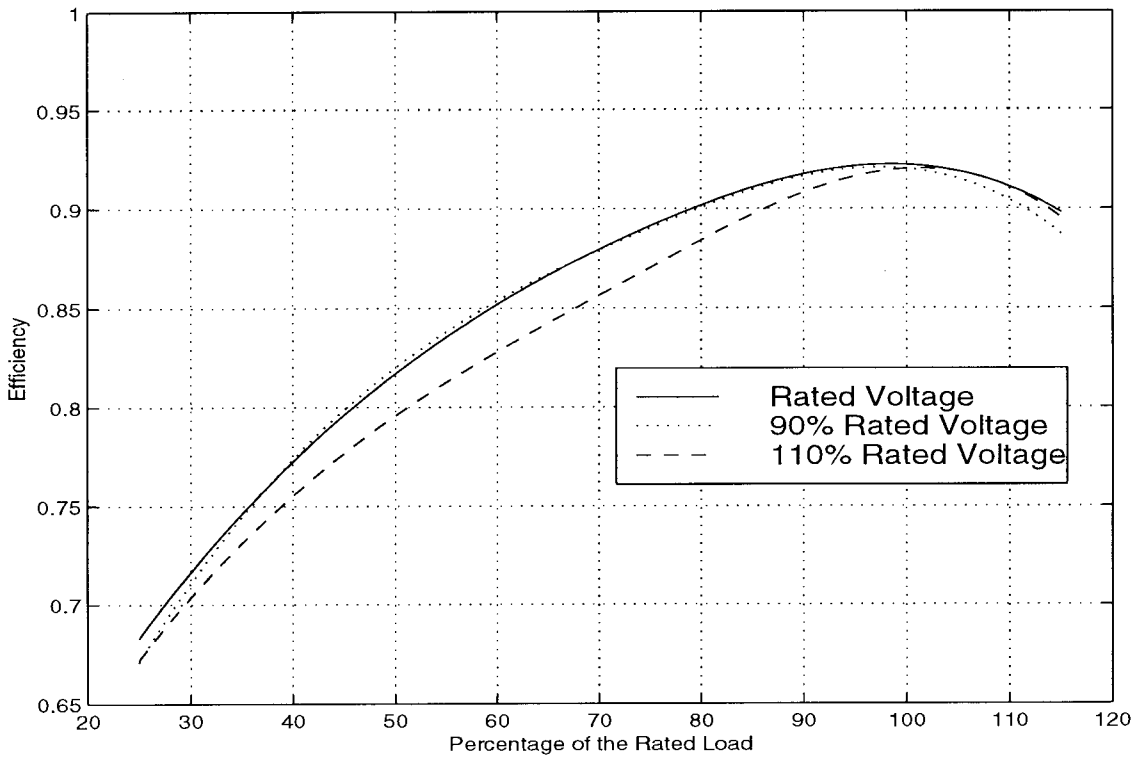

FIGURE 3.7: Voltage Variation effect on Efficiency

rev/min, and, after the power is restored, the current drawn does not exceed 2.1 pu as the machine returns to synchronism (3600 rev/min).

3.7. Voltage Sag Test

In the case of remote locations, voltage sags are seen more often than in a strong line, hence the need to simulate such voltage sags during the testing of the motor.

A sudden voltage sag is not obtainable with the autotransformers which were feeding the WPM, since they have a slow tap changing speed, especially in large

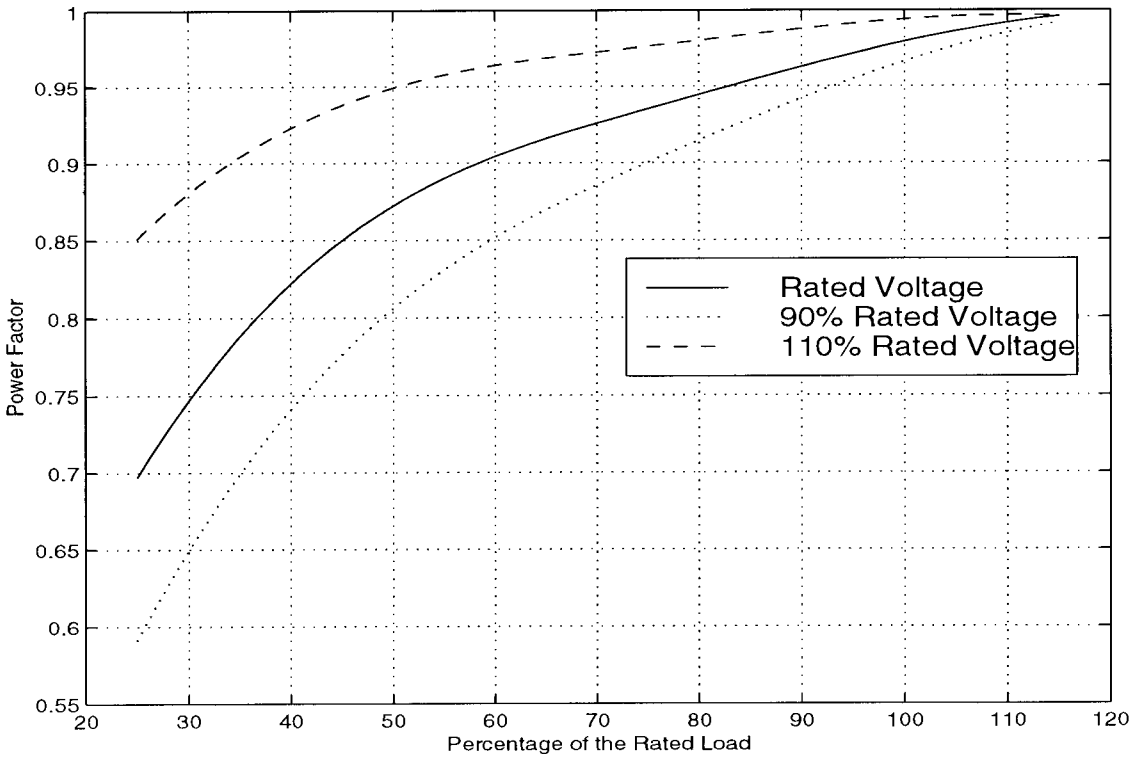

FIGURE 3.8: Voltage Variation effect on Power Factor

variations as needed for this test. The easiest way to simulate a voltage sag was to insert a very low resistance in the input circuit for the WPM, which was short-circuited for the normal operation. The short circuiting switch was opened for the sag condition, where the voltage drop on the resistor accounted for the difference between the voltage available form the source and the voltage at the terminals of the WPM.

The resistor needed in the circuit was sized according to the worst case for the voltage sag. This value was 0.6 ohm at the rated power of the machine (current drawn about 70 A, voltage sag of 20% of 240V). This would account for the additional current drawn by the machine at lower voltage for the same power.

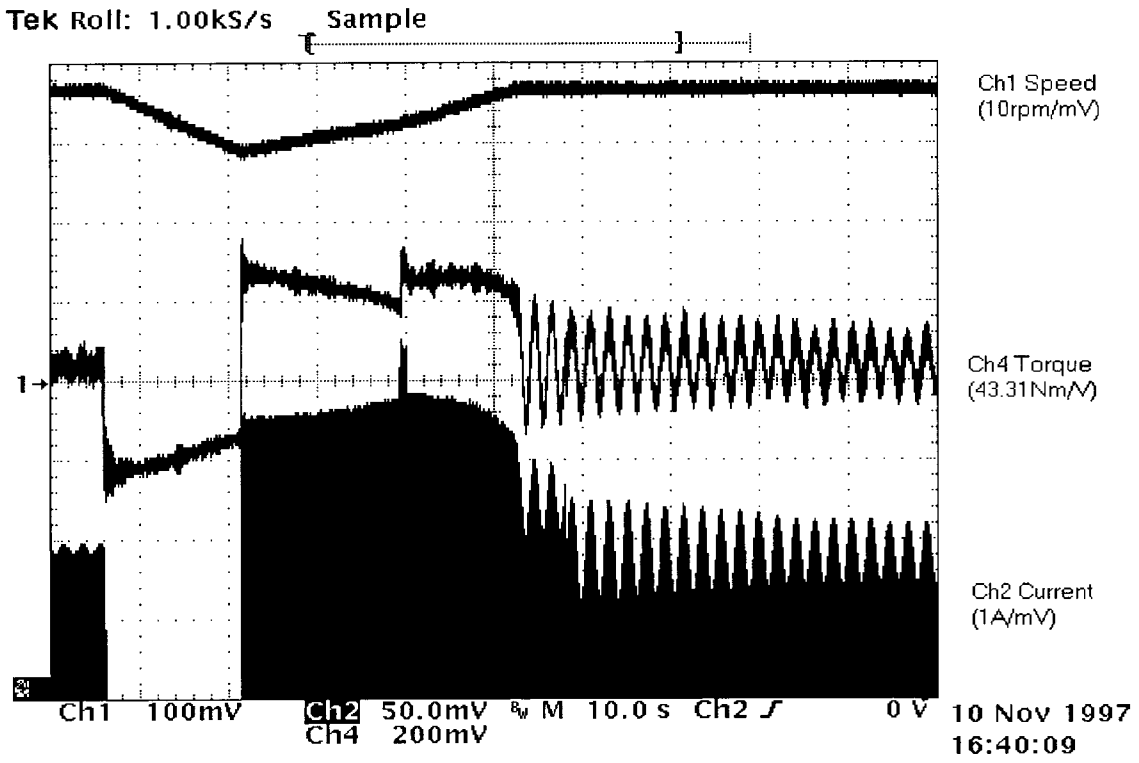

FIGURE 3.9: Rated Load 15 Seconds Power Outage Simulation

At the beginning of the test, the machine was loaded to rated power, its temperature stabilized, and then the voltage sag performed for about 15 seconds. The result if this test is shown in Fig 3.10. The WPM subjected to the voltage sag lost synchronism and its current increased to the level of the starting current. This increase is due to the switching into the circuit of the additional start capacitor (step 2), as well as the pole writing excitation coil becoming energized. Upon removal of the voltage sag, the WPM resynchronizes its load and the current drawn reassumes its pre-fault value. A slight modulation of the available voltage can be observed, which is due to the resistor in the circuit, but still the results are relevant for the field operation of this machine.

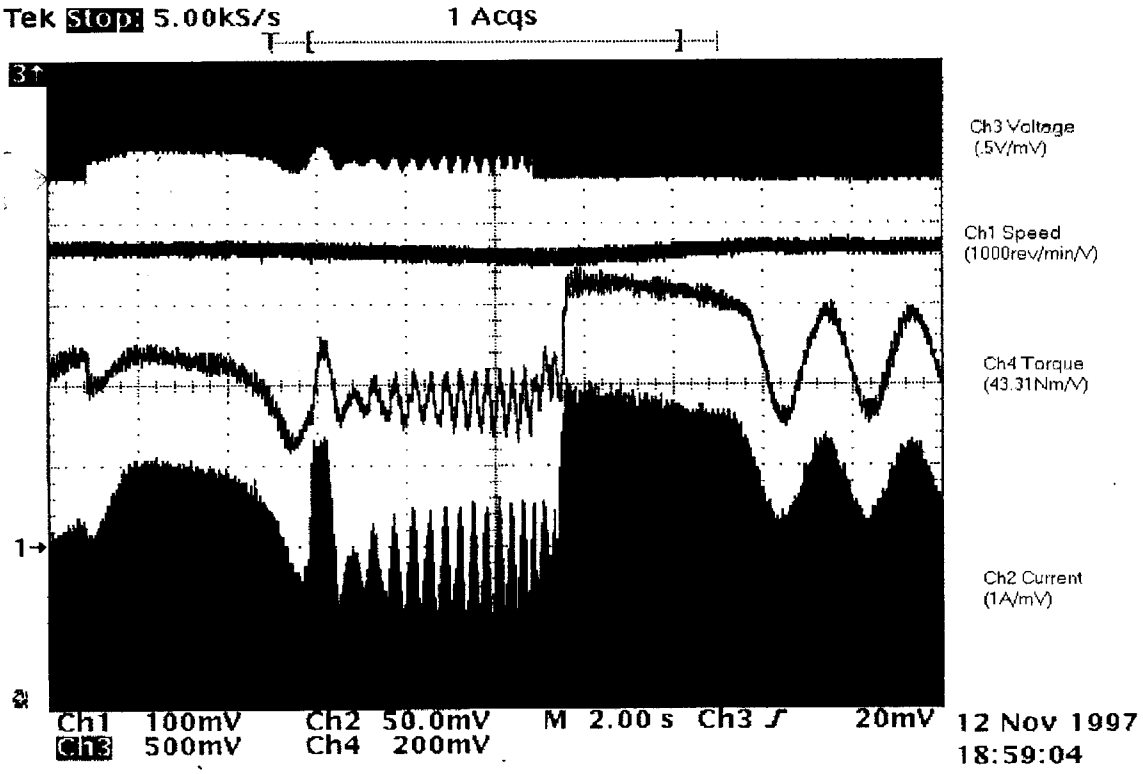

FIGURE 3.10: 20% Voltage Sag Test at Rated Load (15 sec.) and Resynchronization

3.8. Induction Motor Performance and Characterization

3.8.1. Induction Motor Load tests.

For these tests the excitation coil was disabled using the switch available in the control box and the dynamometer was set to speed mode in order to ascertain the torque produced by the machine at different slips. However, the resultant torque is the sum of the IM torque and of the HM torque. There also appears to be some braking torque due to the semi- permanent magnets not being completely erased by the rotating magnetic field of the stator of the WPM. A clear separation of these

components is not readily available. The results of this test are presented in Fig 3.11.

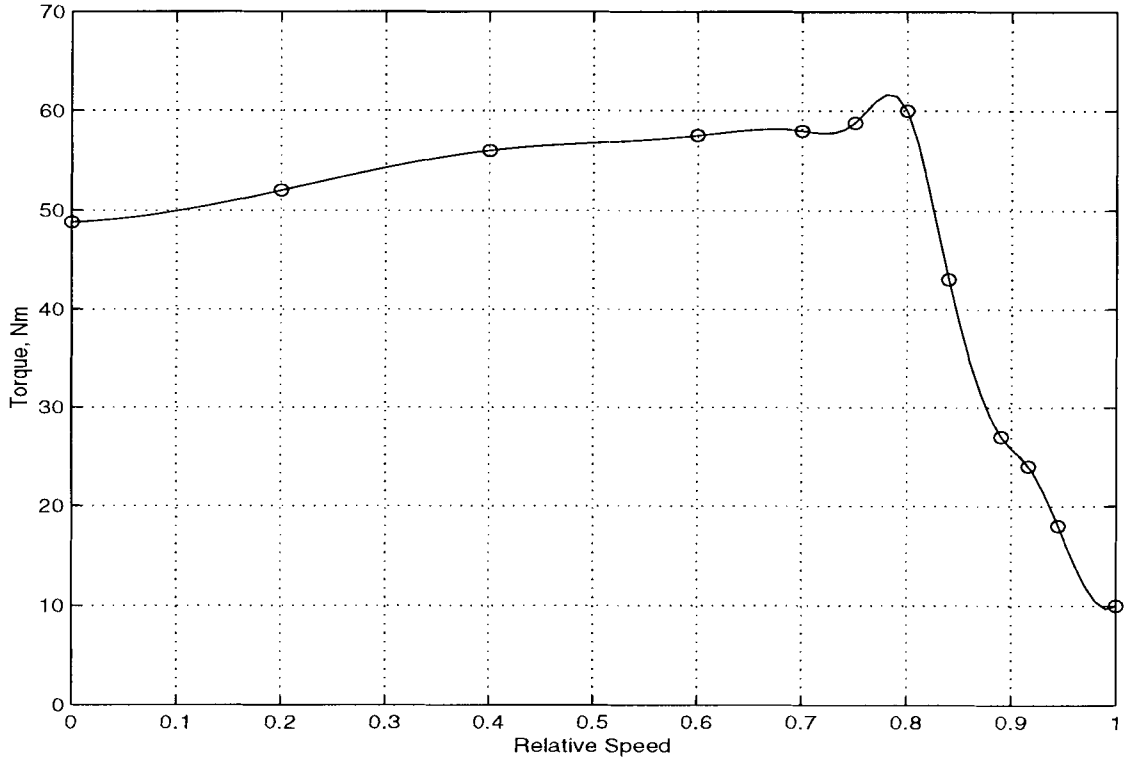

FIGURE 3.11: Steady-State Induction and Hysteresis Resultant Torque

3.8.2. Locked Rotor Tests.

For the locked rotor test, it was feasible for the machine to be energized at rated voltage, due to the very low inrush current (which never exceeds 2.1pu) and to the fact that in normal operating conditions the machine can take up to 5 minutes to start and synchronize its load. This test has been performed both with the motor cold and after the load tests, when the motor was warm.

A significant decrease in the value of the torque and current at the locked-rotor condition was observed when the WPM warmed-up. This reduction can be attributed to the increase of the resistance of the stator windings and rotor cage and to the decrease of the magnetic reluctance of the machine due to the increased thermal motion within the magnetic material of the rotor, and especially of the ferrite ring which seems to be sensitive to temperature variations. The hot locked-rotor torque was 48.6 Nm (122% of the rated torque) whereas the cold test yielded a value of 63 Nm which is about 157.5% of the rated torque of the machine.

3.8.3. Main Winding Tests

The main winding was isolated for testing in the circuit by disconnnecting the auxiliary winding. This configuration eliminates the rotating magnetic field so that there is no torque produced at standstill. However, the magnetic field is sinusoidally distributed in the machine, with a time-varying amplitude modulated at the frequency of the supply (60Hz). The magnetic field can be viewed as the phasor addition of two counter-rotating magnetic fields each with half the amplitude of the real oscillating field. When the machine is driven by external means out of standstill, its behavior towards the two counter-rotating fields changes. Because of hysteresis there is also a delay of the magnetization of the rotor with respect to the inducing mmf wave. Thus, a hysteresis torque, which is a synchronous motor action produced by the angular shift between the axis of rotating primary mmf and the axis of secondary magnetization, is developed [9]. However, the WPM did not produce sufficient torque in order to overcome the friction and the windage of the test system, with the result that the machine did not accelerate towards synchronism or maintain a low slip, but it repeatedly slowed down towards zero speed.

Load Tests

The machine could not be loaded as an induction motor combined with hysteresis motor per se, because the friction and windage of the dynamometer machine exceeded the breakdown torque of the WPM having only one phase connected. In order to investigate the performance of the WPM in this mode, the dynamometer was operated in speed mode and the torque output of the WPM was averaged every time over a period of around 20 seconds in order to get a meaningful result. This was required by the pulsations of the torque exhibited especially at low slips. The torque versus speed characteristic of the main winding section of the motor after using a cubic spline interpolation between the measured points, is presented in Fig 3.12. The motor has been kept at speeds between positive and negative 3600 rev/min in order to investigate the symmetry of the forward and backward rotating field sections of the equivalent circuit. The behaviour was observed to be very symmetrical, this confirming the earlier assumptions that machine can be rotated in either direction with the same performance. It can be seen that the torque is nonzero at synchronous speed. This is due to the following factors: the hysteresis and the superposition of the forward-rotating component of the torque with the backward-rotating one.

Locked Rotor Test

The locked rotor test has been performed at a reduced voltage, for which the controller could not activate the input contactor, thus requiring the input contactor to be manually actuated. The reduced voltage has also the effect of reducing the hysteresis component in the equivalent circuit.

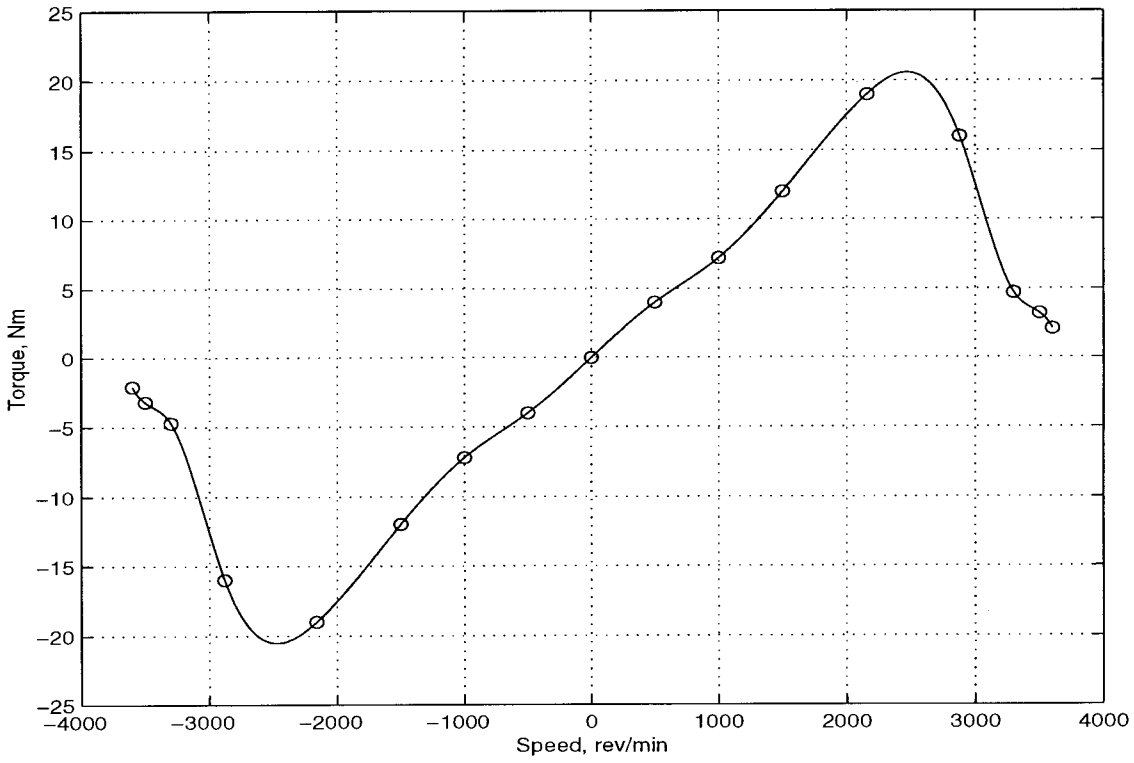

FIGURE 3.12: Main Winding Torque-Speed Characteristic

3.8.4. Auxiliary Winding Tests

The tests performed with the main winding alone were repeated with the auxiliary winding alone in the circuit. In this case the current drawn was significantly higher due to the reduction of the impedance compared to the main winding case, due to the capacitors in the circuit. The resulting torque-speed characteristic are also presented in Fig 3.13.

As we can observe there is a discontinuity around synchronous speed and we can atribute that to the fact that the remanent magnetic poles interacting with the increased current due to the capacitors in the circuit result in a synchronous

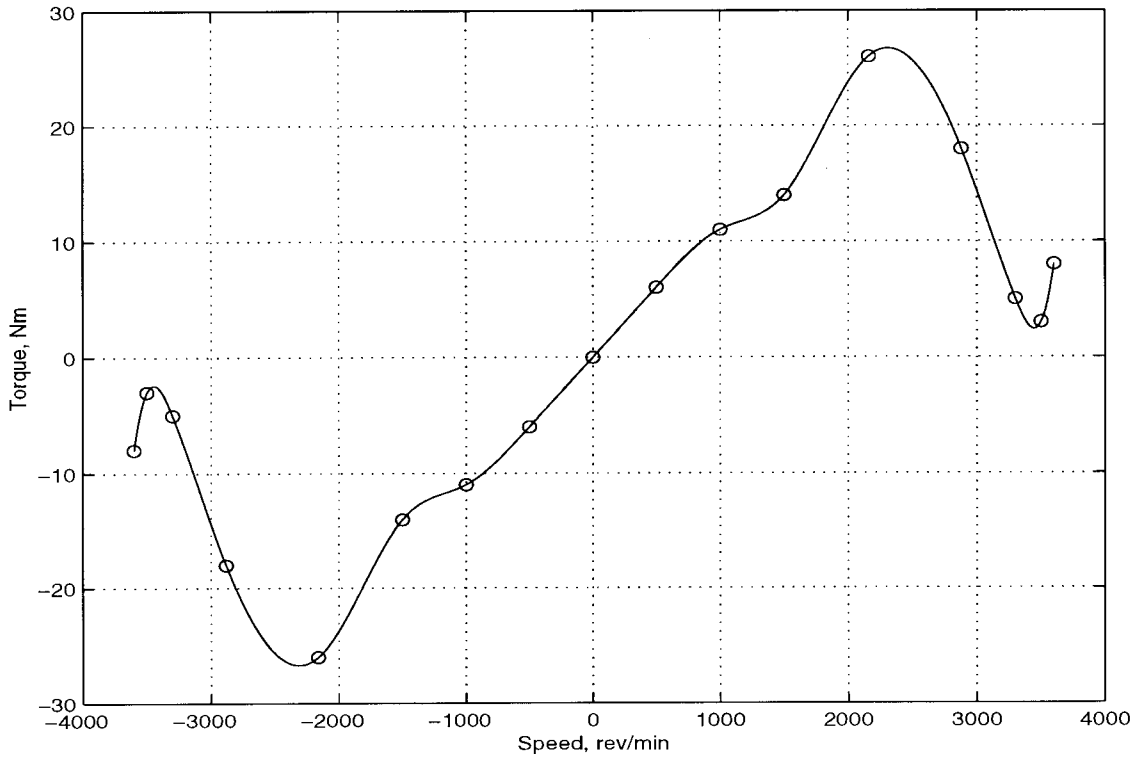

FIGURE 3.13: Auxilliary Winding Torque-Speed Characteristic

component high enough to supply the friction and windage of the test system. This area is obvioulsy not reliable since the WPM experiences a synchronous torque.

3.9. Hysteresis Motor Component Tests

In order to appreciate the hysteresis motor component torque, were the WPM a balanced three phase machine a test could be used involving several equally spaced torque readings at different speeds close to the synchronous speeds. For these tests, the excitation coil should be disabled, so that no poles are written.

An extrapolation towards the synchronous speed of these values would yield the constant component of the torque, which can be assumed to be the hysteresis component for the all modes except the pole writing. This strategy is based on the fact that in a balanced three phase induction machine the torque is zero at synchronism. However, a single phase induction machine exhibits a negative torque at synchronism, the zero torque condition being attained at some subsynchronous speed, close but not equal to the synchronous. Therefore, it is not possible to use this technique for separating the hysteresis and induction torques. This seems to be possible only with a computer based model matching technique, based on several torque points at different speeds. The resulting characteristic, obtained from the torque measurements of the machine without the excitation pole active, and then interpolated for an equal weight in the model matching throughout the speed range was compared with the characteristic of the mathematical model and the parameters of this model were adjusted so that the best fit was obtained. Large pulsations of the torque were recorded at those points and they are attributed to the remanent permanent pole slip.

3.10. Synchronous Machine Tests

For a normal synchronous machine the standard tests involve the open-circuit and short-circuit tests. However, in the case of the WPM there is no way to perform the short-circuit test which involves, in a regular synchronous machine, reduced excitation, at the rated speed.

3.10.1. Open Circuit Test

Immediately following a loaded run of the WPM, when the poles have been freshly written, the WPM was disconnected from its power supply and the dynamometer set in speed mode in order to keep synchronous speed. The open circuit voltage was measured at the main and auxiliary terminals on the motor connection box, without any capacitors in the auxiliary circuit. The recorded open circuit voltage, which, in this case, is equal to the induced emf, having no current in the circuits, was 238V.

3.10.2. Short Circuit Test

In order to pass rated current through the windings, the machine was left to coast down to standstill from the previous experiment and a short circuit was applied initially to each winding and then to all of them together. The WPM was carefully

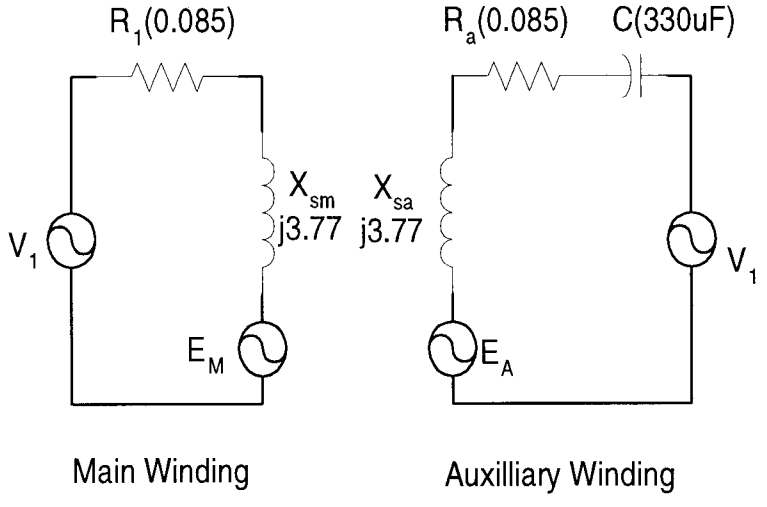

FIGURE 3.14: Permanent Magnet Synchronous Machine Equivalent Circuit

driven by the dynamometer at increasing but slow speeds until rated rms current was observed through the windings. The rated currents were considered to be the currents observed through each winding at rated load. A problem encountered in this test was the fact that the machine produced very low frequencies at the low speeds observed, and the inductive pickups would present large errors. Thus, a Hall effect current probe was used, which is able to accurately measure DC as well as AC currents. The resulting waveform was then integrated on the digitizing oscilloscope in order to find a meaningful rms value. The speed at which the rated current was observed was on average 80 rev/min. The respective frequency was considered in the impedance calculations and the resulting values introduced in the equivalent circuit of Fig 3.14.

4. COMPUTER SIMULATIONS

The WPM was modeled through an equivalent circuit by which its performance can be predicted. The equivalent circuit is an unitary combination of the three aspects of the WPM.

4.1. Quasi Steady-state Model for the WPM

The equivalent circuit of the WPM contains the induction machine component in the form of Veinott's equivalent circuit, in which the synchronous component will be switched on beginning at 80% of the rated speed (2880 rev/min). In addition to these components, the forward and backward rotating halves of the main and auxiliary windings have an additional real element, the hysteresis resistor. The backward rotating part takes into account the hysteresis loss, since at locked rotor condition the two halves of each circuit have the same impedance. Thus the net power developed by the hysteresis torque is zero. During the pole-writing mode the hysteresis torque component does not exist in its proper form because the regime is synchronous, and at synchronism the classic hysteresis torque is zero. This is due to the fact that the rotating magnetic field of the stator windings doesn't sweep the rotor field in order to have a phase difference between the stator mmf and the rotor flux density. However, the hysteresis phenomenon is still present due to the excitation pole. A novel kind of hysteresis torque is developed, which is very difficult to estimate, because of the particular condition; for the first run of the pole-writing around the rotor circumference it will write a sinusoidal permanent magnet flux density profile which will continue for an additional time before reaching the same point on the rotor. The process incurs a hysteresis effect which is proportional to

the remanent value of the flux density. When reaching the reference, starting point, the previously magnetized points on the rotor will be remagnetized to another value, higher or lower, depending on the position of the waveform produced by slip of the machine. This process results in an additional half of a different hysteresis loop. This process is represented in Fig 4.1

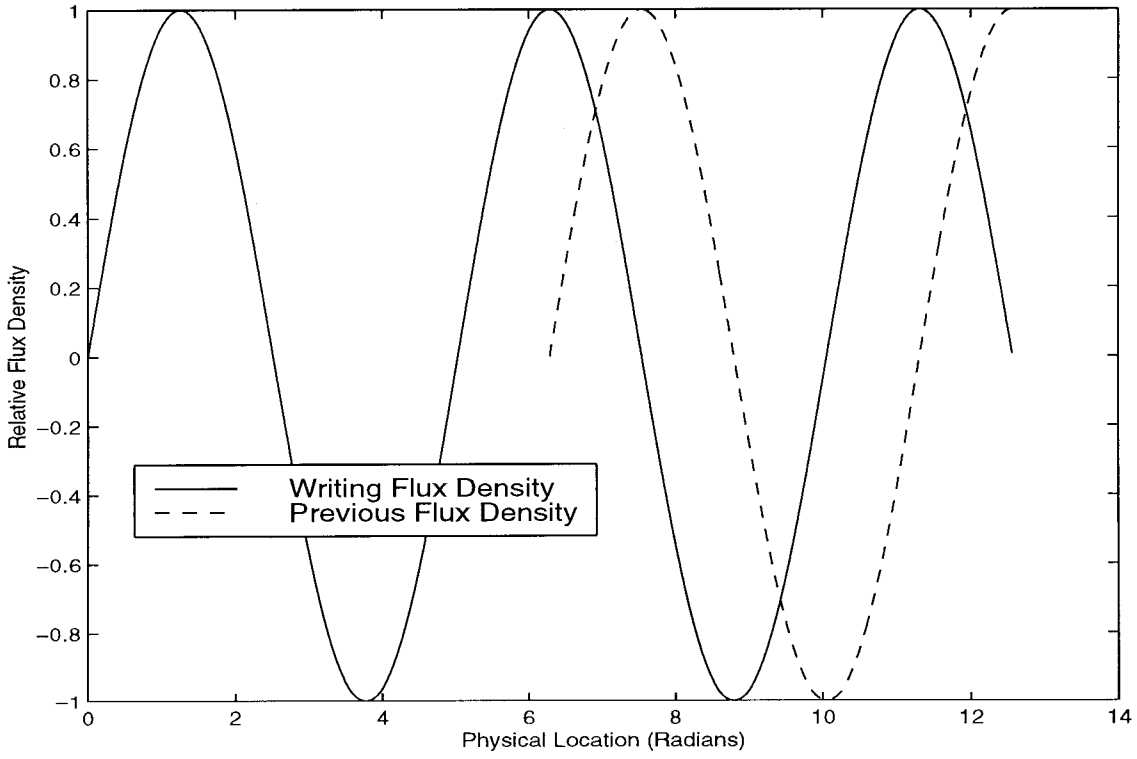

FIGURE 4.1: The First and Second Rotor Circumference Pole Writing Process

A simple solution to this problem reveals a non-linear slip dependence of the hysteresis area covered in a mechanical revolution. Empirical formulas list the hysteresis loss as

$$P_h = k_h \times Vol \times f \times (B_m)^n \tag{4.1}$$

where k_h is a proportionality constant dependent on the magnetic characteristics of the material, Vol is the volume of the material, f is the frequency of excitation, B_m is the maximum value of the flux density and the exponent n ranges from 1.5 to 2.5. It is usual for estimating purposes to attribute a value of 2 to n, which is actually consistent with a square profile of the hysteresis loop as is the case with the ferrite materials. A common approximation in minor hysteresis analysis approximates the minor hysteresis profiles with an ellipse even for the saturated case. In this case their area is proportional with the square of the excursions about the zero mmf point. Therefore, the dependance of the hysteresis area with the slip for a period of the input voltage can be expressed by Eq4.2, which reduces to $8\pi s$.

$$A_{hpw} = \int_0^{2\pi} \mid sin(x) - sin(x - 2\pi s) \mid dx. \tag{4.2}$$

The dependance is difficult to simplify analytically when the upper limit of integration depends on the slip, which is the case when we are interested in the area covered during a mechanical revolution, but its computer generated form is very linear with the slip for the range in question (0 to 0.2). However, the individual points incurr asymmetric hysteresis effects which not yet analytically quantized.

Hence, in the pole-writing mode the hysteresis phenomenon will be represented by a resistor having not a constant value with the slip but one which has a value

$$R_{hpw} = R_h \times 1/s; \tag{4.3}$$

The unknown becomes the constant value R_h which will be determined from curve fitting in a nonlinear system identification fashion.

In order to avoid "divide by zero" errors in the simulaton, the elements containing the slip in the denominator are switched out of the circuit at a slip of 0.1% From 80% to 100% of the rated speed the power angle of the synchronous component equivalent emf is a constant and immediately following synchronization the slip

becomes zero (valid only in the backward-rotating branches) and the load variable becomes the power angle. The equivalent circuit is presented in Fig 4.2.

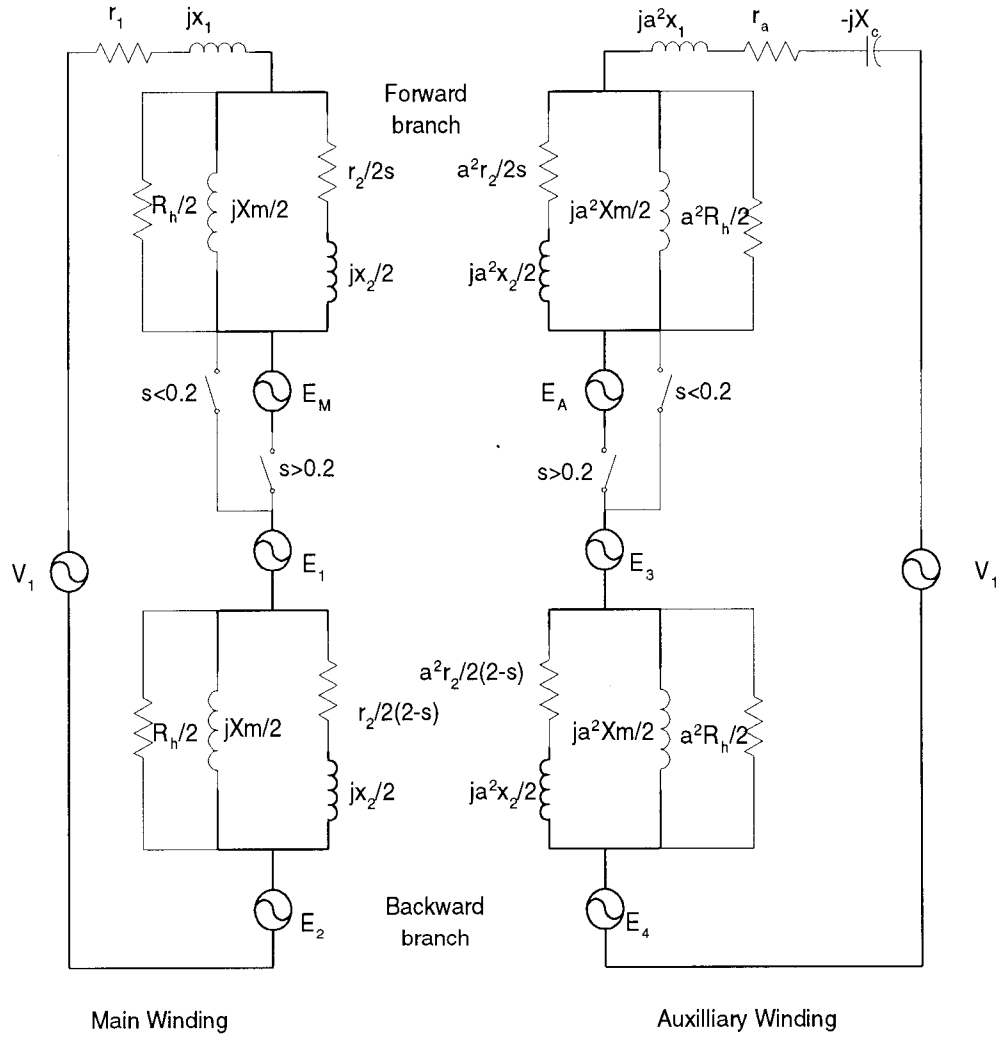

FIGURE 4.2: Single-Phase Written-Pole Motor Equivalent Circuit

This equivalent circuit includes all three components of the WPM:

1. The single-phase induction machine is present in the form of Veinott equivalent circuit having the main and auxilliary circuits, each having a forward and backward rotating half.

2. The synchronous machine is represented, from a slip of 20% on towards the synchronous speed, by E_m and E_a, the back-emfs due to the permanent magnets in each circuit. Their absolute value depends on the actual speed, and they have a relative phase displacement of 90 degrees electrical, in the general case, due to the spatial displacement of the main and auxilliary windings in the machine. In our particular case (for a machine having one pole pair) the mechanical displacement is 90 degrees as well)

3. The hysteresis machine is represented by the resistor R_h which is divided between forward and backward rotating branches just as the cage rotor equivalent resistor. The power dissipated on the forward rotating halves, less that which is dissipated in the backward branches, represents the air gap power. This air gap power, which would be constant in the case of a balanced three phase pure hysteresis machine, is being divided into mechanical power and heat loss in the ratio 1-s:s. Hence, at synchronism, all the hysteresis air gap power is converted into mechanical power, therefore the torque due to this component can be calculated as the ratio of the air gap power to the synchronous speed of the machine. This is valid for all machine modes, with some considerations for the value of the resistor during pole-writing.

4.2. Parameter Optimization

The analytical model of the WPM leaves us with at least two unknown or qualitatively known parameters: The value of the hysteresis equivalent resistor, hence that of the hysteresis torque and the value of the power angle during the pole-writing mode.

In order to get these values, the known parameters in the circuit were substituted in the torque equation along with trial values of the unknown ones and the resulting torque compared with the real torque of the machine in several points. The differences were squared and then added to obtain a cost which was to be minimized by a minimizing subroutine available in Matlab. This approach was dictated by the fact that the torque characteristic is highly nonlinear and the circuit itself is nonlinear as well. The stator and rotor leakage reactances are considered equal in this model and the classical single phase machine theory must be modified to account for the additional real part in the forward and backward parts of the series equivalent circuit used to calculate the induction torque, as shown in Fig4.3. Normally, the

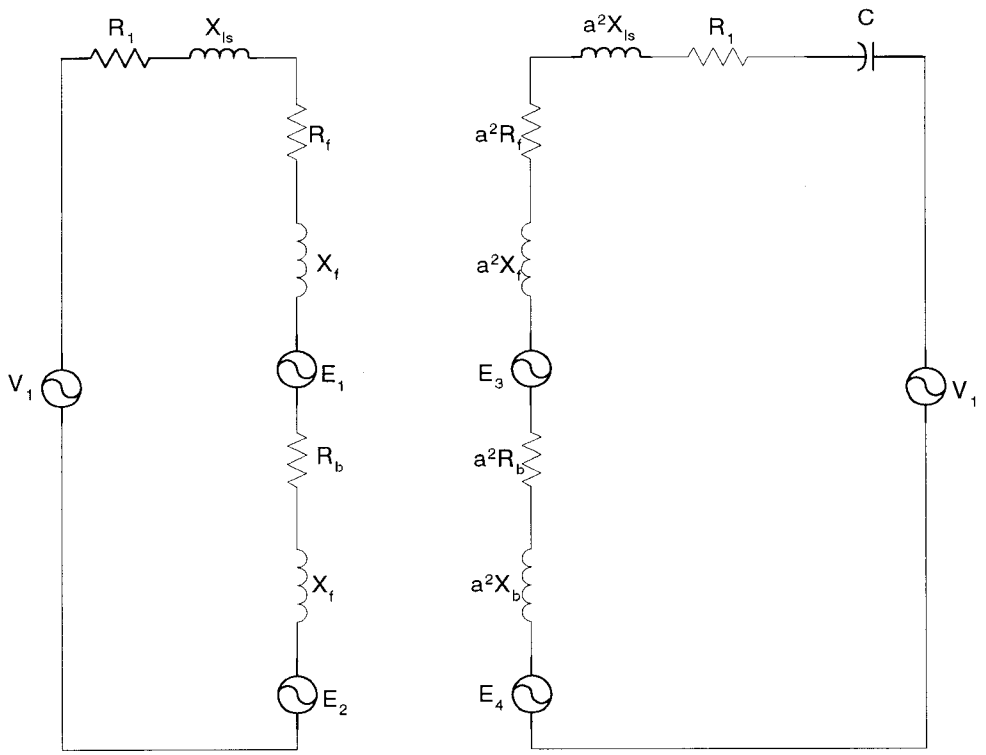

FIGURE 4.3: Series Form of the Single-Phase WPM Equivalent Circuit

induction machine air gap power in the forward rotating branch of the main circuit, for example, is expressed as

$$P_{gfm} = Re[(E_{fm} + E1) \times I_1^*]; \tag{4.4}$$

and so on

$$P_{gbm} = Re[(E_{bm} + E2) \times I_1^*]; \tag{4.5}$$

$$P_{gfa} = Re[(E_{fa} + E3) \times I_2^*]; \tag{4.6}$$

$$P_{gba} = Re[(E_{ba} + E4) \times I_2^*]; \tag{4.7}$$

where the asterisk (*) denotes the complex conjugate. In our case the relationships become

$$P_{gfm} = Re[(E_{fm} + E1) \times I_1^*] - Abs(E_{fm}/(R_h/2)); \tag{4.8}$$

and so on for each branch.

$$P_{gbm} = Re[(E_{bm} + E2) \times I_1^*] - Abs(E_{bm}/(R_h/2)); \tag{4.9}$$

$$P_{gfa} = Re[(E_{fa} + E3) \times I_2^*] - Abs(E_{fa}/(R_h/2)); \tag{4.10}$$

$$P_{gba} = Re[(E_{ba} + E4) \times I_2^*] - Abs(E_{ba}/(R_h/2)); \tag{4.11}$$

The total induction machine air gap power becomes:

$$P_g = (I_1^2 + a^2 I_2^2)(R_f - R_b) + 2a(R_f + R_b) I_1 I_2 sin\theta_{21} - 2/R_h(E_{fm}^2 + E_{fa}^2 - E_{bm}^2 - E_{ba}^2); \tag{4.12}$$

Where the subscripts f, b, m, and a denote forward, backward, main and auxilliary respectively.

The data used in the optimization of the induction and hysteresis components (no pole writing) as well as the resulting torque-speed characteristic of the machine model are presented in Fig4.4. The parameters of the equivalent circuit are com-

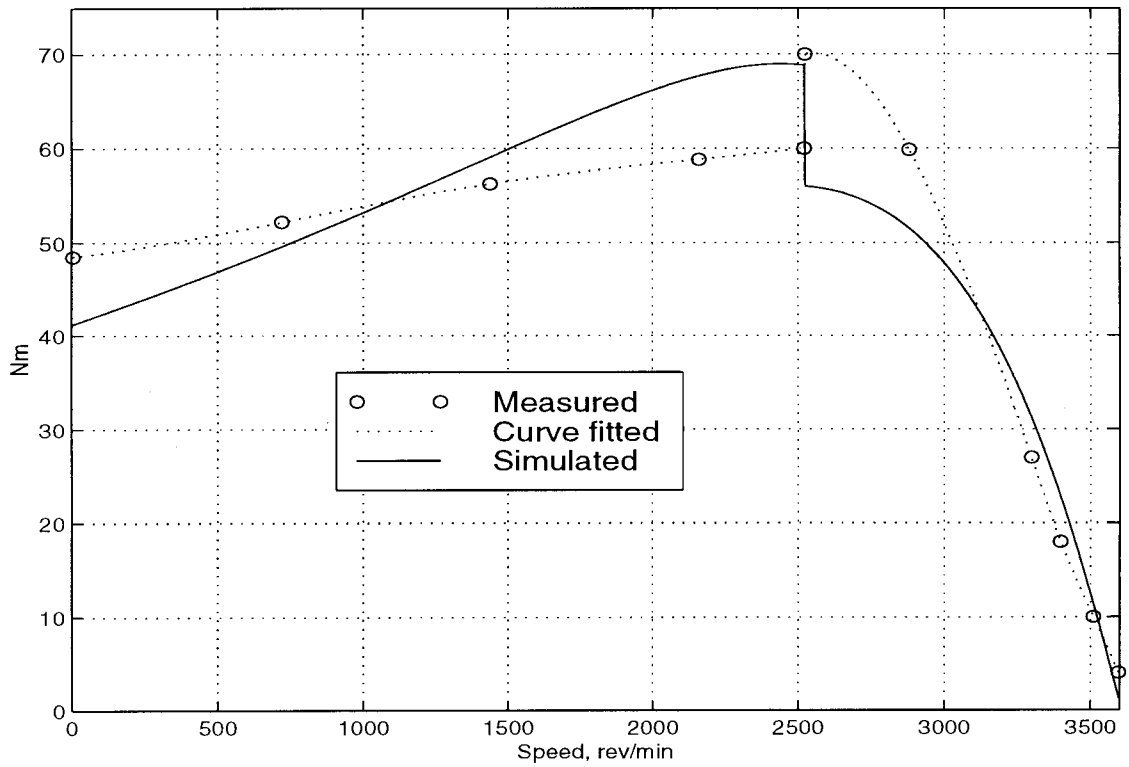

FIGURE 4.4: Comparison of Measured and Model Torques after Optimization

pared with the predicted values in Table 4.1 The parameters resulting from this minimization were reasonably close to the predicted ones. The estimated magnetizing reactance was calculated from the physical dimensions of the machine and assuming a sinusoidal winding distribution and is the closest matched parameter. The rotor resistance turns out to be higher than the predicted value, whereas the predicted leakage reactance was found to be about half the predicted value. The inrush current in the minimized model is slightly lower than the measured value, at 134 A.

The results of this minimization didn't account for any friction and windage, and it is admitted that the data was insufficient for a good fit. The interpolation

	Rotor Resistance	Leakage Reactances	Magnetizing Reactance	Hysteresis Resistor
Predicted	0.35Ω	1.2Ω	6.36Ω	None
Minimized	1.12Ω	.76Ω	5.29Ω	37.25Ω

TABLE 4.1: Comparison of Predicted and Minimized Equivalent Circuit Parameters

given by the cubic splines was not the best, given the nonlinear aspect of the data. The level of complexity of the machine justifies us in considering the results of the optimization acceptable, because of the intricate interaction between the torque producing components of the WPM.

5. CHARACTERIZATION AND PROBLEMS WITH THE WPM

As is apparent from the results of the testing, the WPM turns out to be difficult to understand in detail. The main problem rests in trying to get an in-depth understanding of the interweaving of the induction, permanent magnet, and hysteresis components. During our tests as well as in previous tests conducted by Manitoba Hydro and by the manufacturer itself, one of the problems which is not readily evident is the hunting or dynamic instability of the machine. This phenomenon has been observed at all loads, and seems to be unavoidable with the physical configuration of the machine and the combination of weak induction cage and relatively strong permanent magnet excitation.

This hunting phenomenon requires further investigation not covered in the initial test and analysis plans.

5.1. Overexcited Synchronous Machines

In normal steady state operating conditions a synchronous machine will operate at a fixed load angle, defined as that between the peak of the rotating magnetic field of the armature and the magnetic rotor axis. As the load torque changes, the load angle must be modified to meet the new condition. It is known from the elementary theory of electric machinery that a synchronous machine without damper windings exhibits dynamic instability or overstability or negative damping when one or more of the following are true [5]:

1. The machine is overexcited.

2. The machine is operating at large values of the load angle, δ_0.

3. The machine has a high value of the armature resistance.

5.2. Hysteresis Motor

In general, a hysteresis motor includes eddy-current effects. However, due to the laminar structure of the rotor and the sintered powder nature of the ferrite, eddy-current effects are negligible in the case of WPM. Hence it is valid to consider an ideal hysteresis motor in the following analyses. It is well known that a typical hysteresis motor has a constant torque versus speed characteristic. In the case of a single-phase machine the torque will vary with the capacitance in the circuit, because of modified current through the auxiliary winding.

However, this would induce us into believing that there is a discontinuity about the synchronous speed point.

The hysteresis torque-speed characteristic is actually irrelevant at synchronism, where the characteristic should be expanded to show another parameter, similar to the load angle in a synchronous machine, which should take into account the oscillations of the machine around the stable operating point. In the case of a hysteresis machine the ideal synchronous operation eliminates the hysteresis and the machine operates as a permanent magnet synchronous machine. However, as soon as the load angle is changed, there appears a small hysteresis effect, based on an elliptical B-H curve up to the saturation point. The area of the ellipse is proportional to the square of the change in mmf. In a WPM the magnetic material is permanently magnetized by the writing pole energized at the supply frequency, thus it is subjected to a sinusoidally time-varying mmf. The resulting remanent flux density in the ideal case would be sinusoidally distributed, but having a slight phase shift with respect to the writing mmf. In reality the flux density will have space

harmonics around the rotor circumference. These higher harmonics would actually have an additional beneficial effect on the torque production.

During a small deviation cycle from the steady-state load angle, each point of the rotor circumference would suffer an elementary hysteresis which follows an elliptic path. These paths do not enclose equal areas and they depend on the starting point. This poses major problems in getting a thorough insight into the WPM.

The overstability or dynamic stability of the WPM poses some problems in the following areas:

1. The efficiency of the machine is affected because there is a hysteresis effect associated with the oscillations around the ideal stable point. This leads to unnecessary warming of the rotor layer and it can lead to a loss of the magnetic properties if the temperature increases over the Curie point. During testing, results were taken at the closest point to true "stable" operation (i.e. for a minimum amplitude of the modulating oscilations to appear). Only then was averaging and recording of the data performed. Thus, measurements obtained are prbably slightly optimistic for evaluation of the efficiency.

2. Some applications may require a rigorously constant speed and, for certain load torque profiles, the oscillations of the WPM might resonate with mechanical systems causing beats which might increase in amplitude. This could result in desynchronization the WPM at loads close to the rated load (note that the maximum load recommended for the WPM by the manufacturer is 115% because the WPM reverts to the pole-writing mode in order to compensate for loads in excess of 125%).

3. The shaft may not withstand the increased torsional stress and it may shear due to fatigue if a sufficient factor of safety could not be introduced into the

design. It should be remembered here that, due to the non-conventional mechanical design of this machine, the length of the shaft subjected to torsional stress is half the apparent length of the motor.

6. CONCLUSIONS AND RECOMMENDATIONS

6.1. Performance

The WPM proved to deliver most of what its manufacturer promised: high efficiency, high power factor, low starting current, slow acceleration and decelleration during sudden load changes or power supply perturbations.

The measured efficiency of the WPM has been within 1% of the advertised value of 93%. This is very high for a single-phase machine. It also outperforms a three-phase induction machine with the same ratings in the range of loads beginning from 65% of the rated load and up. A disadvantage is that the WPM will not work for extended periods at loads exceeding 125%, whereas the induction machine will tolerate 150% loads for considerable time albeit with a shortening of the insulation life. The power factor of the WPM is remarkably high and would prove beneficial in maintaining the voltage in a long line if it were the dominant load, because it is leading throughout most of the useful range of loads (therefore behaving as a synchronous capacitor).

Unfortunately the machine does not work in the uninterruptable power supply mode in this single-phase configuration at this time. This is because it has a problem commuting the supply of the controller circuit from the line side of the input contactor over to the motor side, where the induced emf of the slowing rotor would provide for it and for the excitation coil. This is needed in order to have a constant frequency at the output of the WPM in the generator mode, when there is no prime mover available at the shaft.

Low starting current appears to be the WPM's strongest selling point, its value of 2.1pu gives the machine the advantage to be the only choice currently available

without the use of power electronics, which a lot of remote applications users resent at this time.

The external rotor configuration provides more than adequate load ride-through in either reduced voltage or loss of supply conditions. In addition it enables run-up as the inertia is sufficient to overcome the cogging torque present at submultiples of the synchronous speed due to the braking torque of the semi-permanent magnets which are not completely erased during start up.

The cost of the machine, even though higher than some other options available is justified at this time by the very high quality of the mechanical workmanship and the low series production runs.

6.2. Problems

The WPM at this time presents some minor problems:

6.2.1. Dynamic Instability

The WPM does not operate in precise synchronism: hunting, dynamic instability or overstability seems to be the biggest problem of the WPM at this time. This seems to be due to the fact that the machine in the synchronous mode of operation is overexcited and its induction motor cage, which fulfills the role of amortisseur in the synchronouos mode of operation, is too weak to dampen the resulting oscillations. The cage is "weak" because of its relative high resistance and also because of the large effective air gap due to the ferrite layer located on the rotor, between the stator and the rotor laminations. The overexcitation of the machine might stem from the fact that the WPM is an offshoot of the Written Pole Technology which

started primarily with uninterruptible power supply applications. In these applications, a higher induced emf is necessary for the generator mode of operation.

Another cause for the hunting of the WPM during synchronous operation is the high minor hysteresis of the ferrite layer, which is a non-linear effect for anything over 2 deg of deviation from the equilibrium condition [3]. It should be noted, however, that in many applications the hunting, which is less than 0.1% of the synchronous speed, would not be noticeable.

6.2.2. Cogging

As in any typical permanent magnet machine, the WPM exhibits a permanent magnet braking torque at subsynchronous speeds, due to the written poles of the previous operation not being completely erased by the rotating magnetic field. This cogging torque would not be a problem if the machine would go through these speed points faster but, as its acceleration is so low, it tends to dwell there, and, even in the experience of the manufacturer, with the wrong choice of capacitor switching point, might "catch" there and not speed up. An added problem at these points is the length of the shaft, which results in increased elastic deformation.

6.2.3. Shaft Dimension

The shaft of the WPM is designed to match the load machine of the same rating and therefore, if it has the same diameter inside the motor might prove to be subjected to excessive stress because it has a length a considerably greater than comparably sized standard machinery. The length of the stressed section of the shaft is half of the motor length plus the exposed part. During sudden overloads

the inertia of the WPM will exert a high torque spike on the shaft; also the cogging condition and the hunting present at synchronous run subject the shaft to fatigue.

6.3. Recommendations

As added results of the research here are some recommendations for the improvement of the WPM:

6.3.1. Dynamic stability

The dynamic instability of the WPM might be aleviated by redesigning the excitation coil to bring the equivalent permanent magnet excitation down to lower levels, which would eliminate the overexcitation of the synchronous machine component of the WPM, or better yet, since the permanet remanent flux density is directly responsible for the value of the torque in the synchronous mode, by redesigning the stator coils. Future research of the WPM should investigate the behaviour of the machine in steady-state synchronous mode of operation. The excitation should be performed at rated voltage as well as lower or higher levels. Then the voltage levels should be varied and the behaviour of the machine recorded. Improved dynamic stability at higher voltage than the writing voltage would validate our presumption that the machine is indeed overexcited. No passive solution is envisioned for the hunting due to hysteresis without changing the semi-permanent magnet material layer itself. There are active solutions to the hysteresis hunting which might work with the WPM, but that would defeat its purpose of eliminating the electronics in the power path. One possibility is to investigate the effectiveness of an active filter, placed in the supply path.

6.3.2. Cogging

The solution envisioned for the cogging problem of the WPM, which is probably the major obstacle to the development of a physically conventional WPM (internal rotor, low inertia), is the "writing" of poles onto the rotor for the first 5 turns of the start-up of the motor. This is equivalent to a proper demagnetization of the magnetic layer through gradually reduced hysteresis cycles connected to each other, because of the finite pitch of the excitation pole piece and the very low speeds at start. This operation will subject the rotor to increasing amplitude hysteresis cycles followed by decreasing ones due to the fringing effect and the long effective air gap.

6.3.3. Shaft size

The problems stemming from the mechanical design of the machine might be solved by trying a single cup rotor configuration where the shaft is connectted to the bottom of the cup thus having a much reduced length. This might have the result of an increased rotor diameter (for the same inertia and radial play at the end of the cup) and thus of reduced number of applications due to the increased frame size (shorter length and larger diameter).

7. LIST OF ABBREVIATIONS

7.1. General Abbreviations

The following general abbreviations have been used in this thesis:

MSRF - Motor Systems Resource Facility

EPRI - Electric Power Research Institute

WPM - Written-Pole Motor

IEEE - Institute of Electrical and Electronic Engineers

BPA - Bonnevile Power Administration

7.2. Nomenclature

The mathematical models and equations given in this thesis use the following symbols:

V_1 - Supply voltage

r_1 - Main stator winding resistance

r_a - Auxilliary stator winding resistance

X_1 - Main stator winding leakage reactance

X_m - Main winding magnetizing reactance

X_2 - Equivalent main circuit rotor leakage reactance

r_2 - Equivalent main circuit rotor resistance

$E1$ - Voltage induced by the auxilliary forward rotating branch into the main winding forward rotating branch

$E2$ - Voltage induced by the auxilliary winding backward rotating branch into the main winding backward rotating branch

$E3$ - Voltage induced by the main winding forward rotating branch into the auxilliary winding forward rotating branch

$E4$ - Voltage induced by the main winding backward rotating branch into the auxilliary winding backward rotating branch

T_H - Hysteresis torque

A_h - Area of the hysteresis curve

p - number of poles of the machine

emf - electromagnetic force

E_M - Permanent magnet induced emf in the main winding of a synchronous machine

E_A - Permanent magnet induced emf in the auxilliary winding of a synchronous machine

T_S - Synchronous torque

I_M - Main circuit current in a synchronous single-phase machine

I_A - Auxilliary circuit current in a synchronous single-phase machine

P_h - Power being converted into hysteresis

f - Frequency

B_m - Maximum value of flux density.

k_h - Proportionality constant in the hysteresis power equation

A_{hpw} - Area between the previous flux density and the writing flux density for a period of the input voltage during pole-writing

s - slip of the machine

R_{hpw} - Effective hysteresis equivalent resistance during pole-writing mode

R_{eh}- Hysteresis equivalent resistance during pole-writing mode

R_h - Hysteresis equivalent resistance

a - Turns ratio between the main and auxilliary windings.

P_{gfm} - Air gap power in the forward main branch of the equivalent circuit

P_{gbm} - Air gap power in the backward main branch of the equivalent circuit

P_{gfa} - Air gap power in the forward auxilliary branch of the equivalent circuit

P_{gba} - Air gap power in the backward auxilliary branch of the equivalent circuit

E_{fm} - Voltage drop on the forward branch of the main circuit

E_{bm} - Voltage drop on the backward branch of the main circuit

E_{fa} - Voltage drop on the forward branch of the auxilliary circuit

E_{ba} - Voltage drop on the backward branch of the auxilliary circuit

R_f - Equivalent resistance for the forward main rotating branch of the series equivalent circuit of a single-phase machine.

R_b - Equivalent resistance for the backward main rotating branch of the series equivalent circuit of a single-phase machine.

B - Magnetic flux density

H - Magnetic field intensity

APPENDICES

A Name Plate Data for the Single-phase Written Pole Motor

Manufacturer: Precise Power Corporation

Model No.: ME 210020

Serial No.: 125

Rated Power: 20horsepower (15kW);

Phase: 1

Hertz: 60

Rev/min: 3600

Rated Current: 67A;

Rated Voltage: 240V;

Inrush Current: 140A;

Duty: Continuous

Frame: 365Y

Power Factor: 1

Rotor Inertia: $5.77kg \times m^2$

Max. Inertia Load: $6.32kg \times m^2$

B Matlab programs used in modeling the WPM

% This is the file which will call on the minimization subroutine which will call

% on the equation solver to get the behaviour of the model for the parameters

%to be optimized.

%The parameters initialization is done here.

global TT Z;

```
load sample
sample1=sample(1:5);
sample2=sample(6:11);
xi1=1:1:700;
x1=[1 200 400 600 700];
xi2=701:1:999;
x2=[701 800 916 944 975 999];
for i=1:700
      Z(1:700)=spline(x1, sample1, xi1);
end
for i=701:999
      Z(701:999)=spline(x2, sample2, xi2);
end
X0=[32 .9 2 .25 .46];
xoptim=fmins('wpmcost', X0)
save xoptim;
%plot (TT);
%(curve(:,1), curve(:,2)));
hold on;
plot (sample);
%This is the subroutine which calculates the cost associated with the fitting of the
model having parameters given in the input vector X to the experimental data
%s is the slip of the machine
%S is the index of the loop
%omegas=synchronous speed in rad/sec
%a=turns ration between main and auxiliary windings
```

```
function y=wpmcost(X);
global Zf Zb curve I Z;
V1=240;      %Input Voltage
Rh=X(1)      % Hysteresis Equivalent Resistance
Rr1=X(2)     %Rotor Resistance
Rr2=X(5)
Rs=.085;     %Stator Resistance
Xls=X(4)     %Stator Leakage Reactance
Xmag=X(3)    %Magnetizing Reactance
a=1;     %Main to Auxilliary Turns Ratio
omegas=2*pi*3600/60;     %Synchronous Angular Speed
R1=Rs;
ra=R1;
Xlr=Xls;     %Rotor Leakage Reactance
Z1=R1+j*Xls;
%delta=X(5)      % Load Angle of the Synchronous Machine Component During
Pole Writing

     %H=X(5)      % Value of the Hysteresis Equivalent Resistor for Slip = 0.2
for S=1:999;
     if S¡=700;
          Xc=-1/(.00066*2*pi*60);
          Rr=Rr1;      % First Capacitor Step
     else
          Xc=-1/(.00055*2*pi*60);      % Second Capacitor Step
          Rr=Rr2;
```

```
    end
s=1-S/1000;     % Slip
I(:,S)=hmodel(s,Z1,Xmag,Xc,Rr,Xlr, Rh);
prod12=abs(I(1,S))*abs(I(2,S));
prod1=(abs(I(1,S)))^2;
prod2=(abs(I(2,S)))^2;
Rf=real(Zf);     % Forward Branch Resistance
Rb=real(Zb);     % Backward Branch Resistance
Efm=abs(I(1,S)*Zf);     % Voltage Drop on the Forward Main Circuit Branch
Efa=abs(I(2,S)*Zf);     % Voltage Drop on the Forward Auxilliary Circuit Branch
Ebm=abs(I(1,S)*Zb);     % Voltage Drop on the Backward Main Circuit Branch
Eba=abs(I(1,S)*Zb);     % Voltage Drop on the Backward Auxilliary Circuit Branch
E1=I(9,S);     % Induced EMF in the Equivalent Circuit
E2=I(10,S);     % Induced EMF in the Equivalent Circuit
E3=I(11,S);     % Induced EMF in the Equivalent Circuit
E4=I(12,S);     % Induced EMF in the Equivalent Circuit
SumE2=Efm^2+Efa^2-Ebm^2-Eba^2;     %Sum of Voltages squared used in the Calcu-
lation of the Hysteresis Torque
% if S¡=975;
TS=0;
%else
% Rh=H*s;
% TS=syncseries(S,Z1,Xc, Zf, Zb, delta,E1,E2,E3,E4);
%end
Pag(S)=((prod1+a^2*prod2)*(Rf-Rb)+2*a*(Rf+Rb)*prod12*sin(angle(I(2,S))-
angle(I(1,S))));
```

```
NetIMPag(S)=((prod1+a^2*prod2)*(Rf-Rb)+2*a*(Rf+Rb)*prod12*
sin(angle(I(2,S))-angle(I(1,S))))-2/Rh*SumE2;
HT(S)=2/Rh*(SumE2);
TT(S)=Pag(S)/omegas+TS;
end
cost=0;
%keyboard
for in=1:999
cost=cost+(TT(in)-Z(in))^2;
end
y=cost
plot(TT(:));
save I;
save TT;
function y=smodel(S,Z1,Xc,Zf,Zb,delta,E1,E2,E3,E4) V1=240;
ind=.238*S/1091;
[xy]=pol2cart(delta,ind);
EM=x+i*y;
delta2=delta+pi/2;
[x2y2]=pol2cart(delta2,ind);
EA=x2+i*y2;
IM=(V1-EM-E1-E2)/(Z1+Zf+Zb);
IA=(V1-EA-E3-E4)/(Z1+Zf+Zb+j*Xc);
y=(abs(IM)*abs(E1)+abs(IA)*abs(E2))/120/pi;
function y= hmodel(s, Z1, Xmag, Xc, Rr, Xlr, Rh);
%function y= model2(s, Z1, Xmag, Xc, R2, Rr, Xlr, Rh);
```

```
global Zb Zf;
V=240+0i;
R1=real(Z1);
Xls=imag(Z1);
Yf=2/Rh+1/(j*Xmag/2)+1/(j*Xlr/2+Rr/(2*s));
Zf=1/Yf;
a=1;
Yb=2/Rh+1/(j*Xmag/2)+1/(j*Xlr/2+Rr/(2*(2-s)));
Zb=1/Yb;
R2=R1;
Za=R2+j*Xc;
Z(1,1)=Z1+Zf+Zb;
Z(1,2)=-j*a*(Zf-Zb);
Z(2,1)=j*a*(Zf-Zb);
Z(2,2)=Za+a^2*(Zf+Zb+j*Xls);
i1=V*(Z(2,2)-Z(1,2))/(Z(1,1)*Z(2,2)-Z(1,2)*Z(2,1));
i2=V*(Z(1,1)-Z(2,1))/(Z(1,1)*Z(2,2)-Z(1,2)*Z(2,1));
E1=-j*a*i2*Zf;
E2=j*a*i2*Zb;
E3=j*a*i1*Zf;
E4=-j*a*i1*Zb;
J=[i1 i2].';
m=[1 1;
1 1];
m(1,1)=Z1+.5*(Zf+Zb);
m(1,2)=-j*a*.5*(Zf-Zb);
```

```
m(2,1)=j*a*.5*(Zf-Zb);
m(2,2)=Za-.5*a^2*(Zf-Zb);
i(1:2)=J(:).*Zf/(j*Xlr/2+Rr/2/s);
i(3:4)=J(:).*Zb/(j*Xlr/2+Rr/2/(2-s));
y=[i1 i2 i(1) i(2) i(3) i(4) Zf Zb E1 E2 E3 E4].';
```

BIBLIOGRAPHY

1. Shabam A. and Mar D.B. A low-cost single-phase high-efficiency motor. *IEEE Trans. on Energy Conversion*, 7(3):560–569, Sept 1992.

2. Wallace A.K., von Jouanne A., and Rollman T. A fully regenerative high-power testing facility for motors, drives and generators. In *IEEE International Electric Machines & Drives Conference record, pp. MB2-13.1-3*, 1997.

3. Stanley P. Clurman. On hunting in hysteresis motors and new damping techniques. *IEEE Transactions on Magnetics*, pages 512–517, 1971. September.

4. Friesen D. and St. George D. Independent laboratory and field tests of a Written-Pole Motor. In *Wescon '96 Conference Proceedings, Anaheim, CA*, Oct 1996.

5. Levi E. *Polyphase Motors, A Direct Approach to Their Design.* John Wiley & Sons, 1984.

6. McPherson G. and Laramore R. D. *An introduction to Electrical Machines and Transformers.* John Wiley & Sons, 1990.

7. Veinott C. G. *Theory and Design of Small Induction Motors.* McGraw-Hill, 1959.

8. Retter G. J. *Matrix and Space-Phasor Theory of Electrical Machines.* Akademiai Kiado, Budapest, 1987.

9. Sarma M.S. *Electric Machines, Steady-State Theory and Dynamic Performance.* Wm. C. Brown, Dubuque, IA, 1985.

10. Smith O.J.M. Three phase motor control. In *US Patent No. 5,300,870*, 1994.

11. Morash R.T.and Roesel Jr. J.F.and Barber R.J. Improved power quality with "Written-Pole"^{TM} motor-generators and "Written-Pole"^{TM} motors. In *Third International Conference on Power Quality: End-Use Applications and Perspectives*, Amsterdam, The Netherlands, Oct 1994.

12. Guru B. S. and Hiziroglu H. R. *Electric Machinery and Transformers.* Harcourt Brace Jovanovich, 1988.

13. Hoffman S. The Written-Pole revolution. *EPRI Journal*, 22:26–35, 1997. May/June.

14. Boldea I.and Nasar S.A. *Linear Motion Electromagnetic Systems.* John Wiley & Sons, 1985.